INVESTIGATING THE ROLES OF IMPORTANT AMINO ACID RESIDUES IN GTPase ACTIVITY OF ELONGATION FACTOR-Tu (EF-Tu)

by

Şeref Gül

B.S., Chemistry, Boğaziçi University, 2008

Submitted to the Institute for Graduate Studies in
Science and Engineering in partial fulfillment of
the requirements for the degree of
Master of Science

Graduate Program in Chemistry
Boğaziçi University

2010

ACKNOWLEDGEMENTS

I would like to express my sincere gratitude to my thesis advisors Prof. Dr. Viktorya Aviyente and Asst. Prof. Bülent Balta for their supervision, patience and invaluable scientific guidance. I would like to thank Prof. Aviyente for her continuous support and encouragement throughout my graduate education years. It was a privilege to be a M.S. student of her. I feel very lucky to get a chance to study with Asst. Prof. Bülent Balta. I learnt a lot from him, I always felt his continuous support and excellent guidance throughout this study.

I would also thank to the members of my committee: Prof. Neşe Bilgin, Prof. Dilek Çalgan and Prof. Pemra Doruker for their valuable advices and comments.

I want to thank all the members of computational chemistry group, to İsa Değirmenci, Tuğba Furuncuoğlu, Gülşah Çifci, Burcu Çakır Dedeoğlu, İlke Uğur, Özlem Karahan, Hasan Hüseyin İnce and Sesil Agopcan, for their friendship and support. I would like to thank all the members of the faculty in Bogazici University Chemistry Department and to all my friends in the Chemistry Department.

It is a great pleasure for me to express my great indebtedness and love to my family for their continuous support and extreme love throughout my life.

ABSTRACT

INVESTIGATING THE ROLES OF IMPORTANT AMINO ACID RESIDUES IN GTPASE ACTIVITY OF ELONGATION FACTOR-TU (EF-TU)

A large number of guanosine triphosphate (GTP)/ guanosine diphosphate (GDP) binding proteins (G-proteins), which usually have intrinsic (and/or stimulated) GTPase activity, are involved in a wide range of cellular regulatory and signal transduction processes. G-proteins generally exist in an active form when bound to GTP and become inactive when GTP is transformed to GDP through a hydrolysis reaction. The longer a GTP-binding protein remains in its active GTP-bound state, the longer it will transmit and amplify a certain signal. The mechanism of GTP hydrolysis is still largely unknown and of great importance to the understanding of the role of specific residues, which may lead to new and novel therapies for cancer.

Experimental studies indicated the significance of some amino acid residues, e.g. His85, Asp87, Asp51, Thr62, Val20 and Ile61, for structural properties and GTPase activity of Elongation Factor-Tu (EF-Tu). In our study we aimed the comprehensive explanations of the roles of these amino acids.

Our results indicated that, Switch 1 area is very unstable and dynamic when introduced into the solvent medium. Early conformational changes of this region in our simulations are showing the flexibility of the Switch 1 area. Thr62 was determined as the key factor for holding the position of Switch 1 region seen in the crystal structures coming from *Thermus aquaticus* and *Escherichia coli* species. On the other hand, Asp51 had no contribution to the position of this region.

Previously, it was proposed that His85 stabilizes GTP hydrolysis transition state by orienting the attacking water molecule, especially in the ribosome induced mechanism. In our study two steps were determined for His85 activity: turning into the active site and to have a stable conformation in this site. We proposed that following factors can help His85 rotation into the active site:

i) Protonation state of itself e.g. if it bears positive charge it has a tendency to stay in the active site more than the neutral form.

ii) Other amino acids can help its stay in the active site e.g. His85 spent more time in the active site in the EF-Tu[D87E] mutant simulation.

iii) Ribosome, probably, may bring and stabilize His85 into active site.

Our findings suggested the stabilization of His85 in the active site could be achieved by Val20 and Ile61 which were previously called as the “Hydrophobic Gate” residues. These residues were thought as the barrier for His85 rotation into the active site. However, our results indicated that the mission of Val20 and Ile61 is not forming a barrier for His85 rotation, but assisting the hydrolysis when it turns into the active site by holding the His85 imidazole ring, preventing its rotation, like a clamp. This stabilization probably mostly happens in the presence of ribosome.

ÖZET

UZAMA FAKTÖRÜ TUNUN GTPAZ ETKİNLİĞİNDEKİ ÖNEMLİ AMİNOASİTLERİN ROLLERİNİN ARAŞTIRILMASI

Guanozin trifosfat (GTP)/guanozin difosfat (GDP) bağlayıcı G-proteinleri GTPaz aktiviteye sahip olup hücre düzenleyici ve sinyal gönderici potansiyelleri vardır. G-proteinleri GTP ye bağlı oldukları zaman aktif olup, GTP nin hidroliz yolu ile GDP ye dönüşmesinden sonra aktivitelerini yitirirler. G-proteinleri GTP ye bağlı kaldıkları süre boyunca sinyal iletmeye devam ederler. GTP ye bağlı G-proteinlerinin hidroliz mekanizması oldukça önem taşımasına rağmen ayrıntılı bir biçimde bilinmemektedir. GTP nin hidroliz mekanizmasının aydınlığa kavuşması spesifik aminoasitlerin bu tepkimedeki rollerini açıklayabilmek, (fazla/az) sinyal iletme esnasında oluşabilecek tümörlerin oluşumunu açıklayabilecek bilgilerin uzun vadede oluşmasında katkıda bulunacağından büyük önem taşımaktadır.

Bulgularımız, *Thermus aquaticus* ve *E.coli* canlılarından gelen kristal yapılarında görülen Anahtar 1 bölgesinin, sulu ortama konduğunda çok hareketli ve kararsız bir yapısının olduğunu gösterdi. Henüz simülasyonlarımızın başında gözlemlediğimiz bu alandaki yapısal değişiklikler, Anahtar 1 bölgesinin ne kadar esnek olduğunu göstermektedir.

Daha önceki çalışmalarda, özellikle de ribozom tarafından tetiklenen GTP hidroliz reaksiyonunda, His85 aminoasidinin saldıran suyu yönlendirerek geçiş konumuna yardımcı olduğu düşünülmekteydi. Çalışmamız His85 in etkinliği için iki adımın gerekli olduğunu gösterdi: Aktif bölgeye dönmek ve burada kararlı bir yapıya sahip olmak. Aşağıdaki faktörlerin His85 in aktif bölgeye dönmesine yardımcı olduğu düşünülmektedir:

i) Protonlanma durumu, örneğin, His85 pozitif yüklü olduğu durumda yüksüz olduğu durumlarına göre daha çok aktif bölgede kalmak istediği belirlenmiştir.

ii) Diğer aminoasitler aktif bölgede kalmasına yardımcı olabilir, örneğin, EF-Tu[D87E] mutasyona uğramış yapısından gelen simülasyonlarda, His85 in daha çok aktif bölgede kaldığı saptanmıştır.

iii) Muhtemelen, ribozom His85 i aktif bölgeye getirip orada kararlı bir geometri kazanmasına yardımcı olmaktadır.

Sonuçlarımız, His85 in aktif bölgede kararlı bir yapıya sahip olmasının, daha önceleri "Su Sevmeyen Kapı" olarak adlandırılan Val20 ve Ile61 aminoasitleri tarafından sağlandığını göstermektedir. Bu iki aminoasit His85 in aktif bölgeye dönmesine engel oluşturduğu düşünülüyordu. Fakat bulgularımız bunların görevinin His85 e bir engel oluşturmak olmadığını, His85 aktif bölgeye dönünce onun imidazol halkasını bir kıskaç gibi tutarak dönmesine engel olup hidrolize yardımcı olmak olduğunu gösterdi. Bu kararlı yapı büyük ihtimalle ribozomun varlığında daha çok açığa çıkmaktadır.

TABLE OF CONTENTS

LIST OF FIGURES

LIST OF TABLES

LIST OF SYMBOLS/ABBREVIATIONS

A_{ij}	Coulomb potential
a	Accelaration
B	Number of times the property is sampled
B_{ij}	Coulomb potential
D	Number of atoms in the system
E	Potential energy
E_b	Energy for bond angle
E_{nb}	Energy for non-bonded interactions
E_s	Energy for bond stretching
E_ω	Torsional energy
F	Force
F(k)	Force vector
f(r)	Conservative force acting on the particle
f′	Random force
h	Planck's constant
k_b	Boltzmann constant
k^b	Force constant for bending
k^s	Force constant for strectching
l	Actual bond length

l_0	Assigned bond length
M	Total number of bond angles
m	Mass
N	Total number of bonds
p	Momentum
q	Phase point
q_i	Partial charge on atom i
q_j	Partial charge on atom j
r_{ij}	Distance between atom i and j
T	Absolute temperature
v	Velocity
v_i^2	Squared velocity of ith atom
x	Position vector in 3N dimensional space
γ	Phase factor
ε	Dielectric constant of medium
ζ	Frictional constant
θ	Actual bond angle
θ_0	Assigned bond angle
λ(k)	Step size
ω	Torsion angle

aa	Amino acid
aa-tRNA	Amino acyl-tRNA
Ala	Alanine
Arg	Arginine
Asn	Asparagine
Asp	Aspartate
ATP	Adenosine triphosphate
Cys	Cysteine
E.coli	Escherichia Coli
EF-Tu	Elongation Factor-Tu
GAP	GTPase activating protein
GBP	GTP binding protein
GDP	Guanosine diphosphate
GEF	GTP/GDP exchange factor
Gln	Glutamine
Glu	Glutamate
Gly	Glycine
GTP	Guanosine triphosphate
GTPase	GTP hydrolyzing enzyme
HID	Imidazole ring of His bears an hydrogen atom on N_{δ}.
HIE	Imidazole ring of His bears an hydrogen atom on N_{ε}.
HIP	Imidazole ring of His bears two hydrogen atoms on both N_{δ} and N_{ε}.

His	Histidine
Ile	Isoleucine
Leu	Leucine
Lys	Lysine
MD	Molecular dynamics
Met	Methionine
mRNA	Messenger ribonucleic acid
PDB	Protein data bank
PMEMD	Particle mesh ewald molecular dynamics
Phe	Phenylalanine
Pro	Proline
RF	Release Factor
Sec	Selenocysteine
Ser	Serine
T. Aquaticus	Thermus Aquaticus
T. Thermophilus	Thermus Thermophilus
Thr	Threonine
Trp	Tryptophan
Tyr	Tyrosine
tRNA	Transfer ribonucleic acid
Ts	Temperature stable
Tu	Temperature unstable

UFF	Universal Force Field
Val	Valine

1. INTRODUCTION

1.1. Role of Elongation Factor in Protein Synthesis

Ribosome synthesizes proteins according to the primary structural information which is encoded in the mRNA nucleotide sequence [1]. Not only ribosome but also some other molecules are involved in protein synthesis, e.g. RNAs, proteins. There are different types of RNAs. One of those which encode the amino acid sequence of protein, called as mRNA. The other group of RNAs which serve as an adaptor, supplying activated amino acids and provide strong convenience between nucleotide triplets and amino acids are called as tRNA. In another group of RNAs which have a regulatory role are called as transport-messenger RNAs. The second group of molecules which participate in protein synthesis are the aminoacyl-tRNA synthetases (aa-tRNA synthetases), translation factors, and numerous accessory proteins involved in regulation of translation. The third group consists of some small molecules: ATP, GTP, amino acids, and various ions [2]. Some of the translation factors have GTPase activity [3]. These factors bind and hydrolyze GTP to GDP at certain steps of protein synthesis. GTP hydrolysis is triggered by the ribosome in a proper functional state. In *Escherichia coli* first of those factors is the initiation factor 2 (IF2), which provides the ribosome with initiator fMet-tRNA^{fMet} [4]. Second ones are elongation factors Tu (EF-Tu) and G (EF-G) that are in charge for binding of a new aminoacyl-tRNA in the A site of the ribosome and translocation, respectively [5-8]. And the final one is release factor 3 (RF3), which releases another termination factor (RF1 or RF2) from the posttermination ribosome complex [9-10].

In our study we will mainly emphasize the GTP conformation of the elongation factor Tu (EF-Tu) and investigate the role of important amino acid residues in GTP hydrolysis in light of the experimental studies by using molecular mechanics tools.

The history of the elongation factor (EF) Tu goes back to 1960s. It was first isolated in 1964 in complex with EF-Ts, the factor T (T=temperature) was classified into two

different classes as temperature unstable (Tu) and stable (Ts) component [11]. EF-Tu belongs to G-protein superfamily. They regulate various cellular activities as a carrier of information or biological components. Common properties of the member of this superfamily are that (a) they cycle between an active and an inactive conformation depending on the nucleotide either GTP (“on” state) or GDP (“off” state) is bound and (b) they have very low intrinsic GTPase and GDP/GTP exchange activity. These two events, that control the level of the functionally active EF-Tu·GTP conformation, are activated by two specific partners in most GTP binding proteins (GBP), generally called GTPase-activating protein (GAP) and GDP/GTP exchange factor (GEF). As far as EF-Tu is concerned these duties are fulfilled by the ribosome and the EF-Ts, respectively [12-14]. GTPases include different proteins such as the well known Ras-like GTPases, translation factors, and GTPases involved in heterotrimeric G-proteins and known as Gα subunits.

In bacterial cells, EF-Tu·GTP carries aminoacyl tRNA (aa-tRNA) to the A site of the mRNA-programmed ribosome carrying peptidyl-tRNA in the P site. EF-Tu in the GTP-bound form has great affinity for aa-tRNAs. The ternary complex, EF-Tu·GTP·aa-tRNA, binds to the ribosomal A-site. Cognate codon-anticodon interaction triggers GTP hydrolysis on EF-Tu (Figure 1.1). After hydrolysis, major rearrangement on the universally conserved switch I (effector loop) and switch II regions were observed. The global change also leads to a great reduction in affinity for aa-tRNA of EF-Tu·GDP complex [15].

The next step in protein synthesis which is controlled by EF-G, is the translocation of peptidyl-tRNA from A to the P site. EF-G moves the discharged tRNA placed in the P site to the E site. Now, vacant A site is ready to start subsequent elongation cycle.

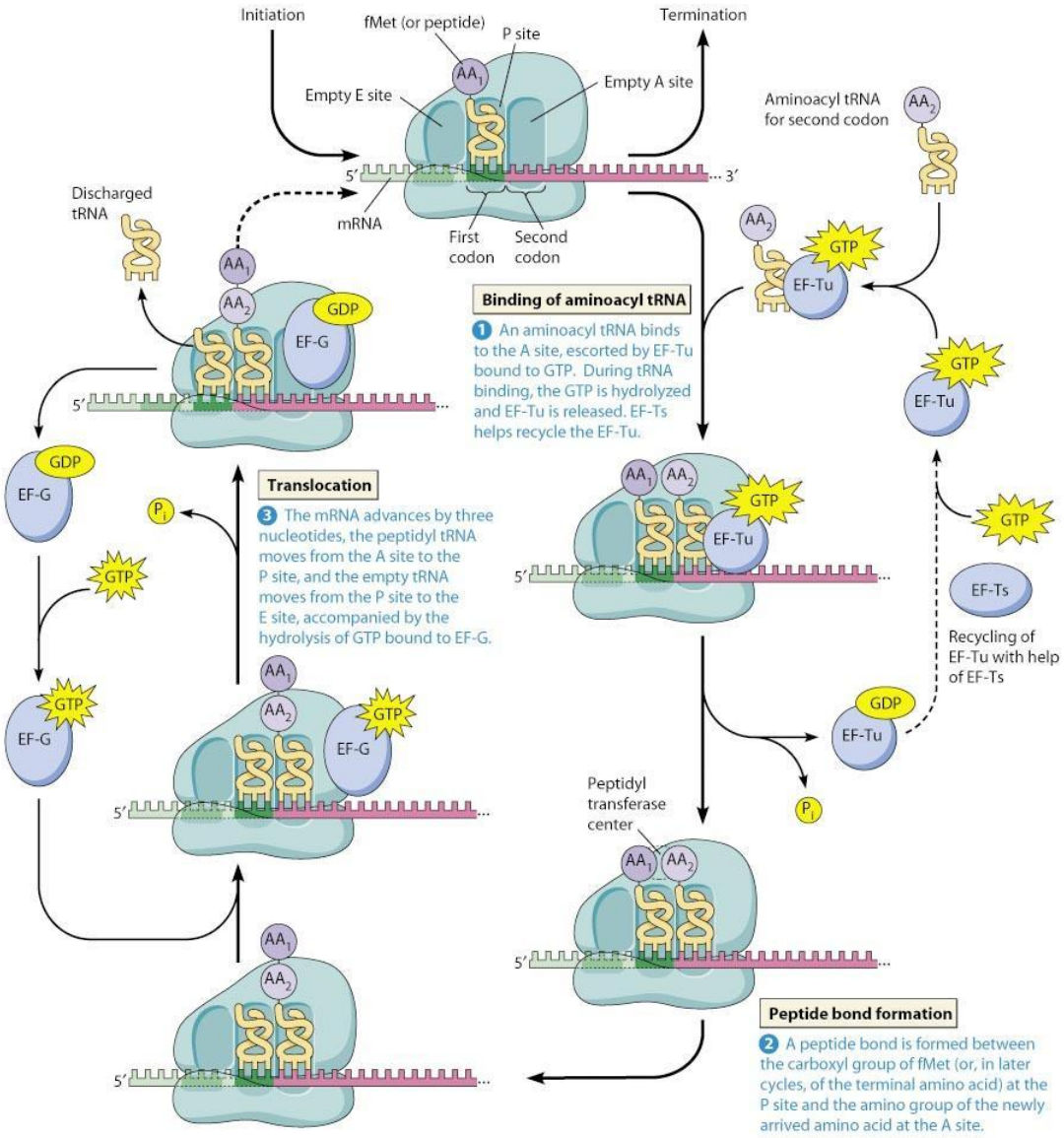

Figure 1.1. Scheme of the EF-Tu function in the elongation cycle of protein biosynthesis [16].

Various factors contribute to the recycling of the released EF-Tu·GDP: (a) the presence of EF-Ts that favors the dissociation of GDP nucleotide from EF-Tu. EF-Ts behaves as a GEF and decreases the affinity of EF-Tu to GDP. GDP dissociates from EF-Tu and it is exchanged with GTP. In the absence of EF-Ts, EF-Tu has two orders of magnitude higher affinity to GDP than GTP and, also, GDP dissociates at an extremely slow rate. The presence of EF-Ts ensures the EF-Tu·GTP form. (b) The interaction

between EF-Tu and aa-tRNA strongly increases the affinity for GTP. (c) The 5- to 10-fold higher concentration of GTP than that of GDP in the cell, also contributes to recycling [12, 17, 18].

EF-Tu alone can hydrolyze the GTP to GDP which is called as the intrinsic GTPase activity of EF-Tu. EF-Tu has very low intrinsic GTPase activity. However some factors may increase the hydrolysis rate such as monovalent cations, vacant ribosome and kirromycin. These factors may increase the rate from 5 to 100 fold. On the other hand, mRNA programmed ribosome with occupied P site is the strongest enhancer of the GTP hydrolysis rate up to 10^5 times faster than that of intrinsic rate [1, 12, 19].

1.2. Structure of Elongation Factor Tu (EF-Tu)

EF-Tu from bacteria and its eukaryotic/archeal counterpart (EF-1α) is a monomeric protein with about 400 amino acids, and a molecular mass of 40-52 kDa. It consists of 3 domains which are known as, Domain I (aa: 1-212), Domain II (aa: 212-310) and Domain III (310-405) (Figure 1.2). Domain I includes the nucleotide binding site. In this study, amino acid numbering is done according to the EF-Tu structure coming from *Thermus aquaticus* species, unless otherwise stated [20, 21].

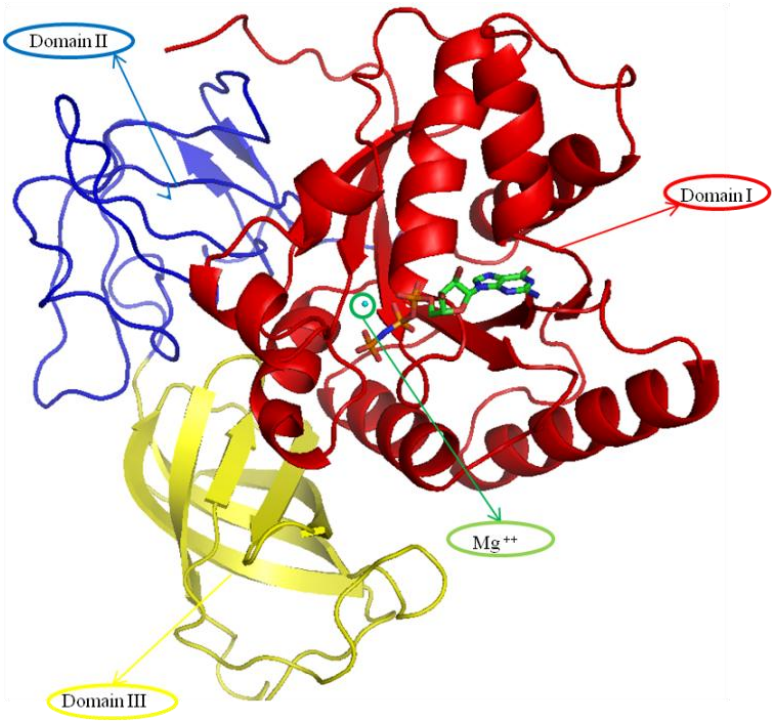

Figure 1.2. Structure of GTP bound EF-Tu (active form) from *Thermus aquaticus* (PDB ID: 1EFT).

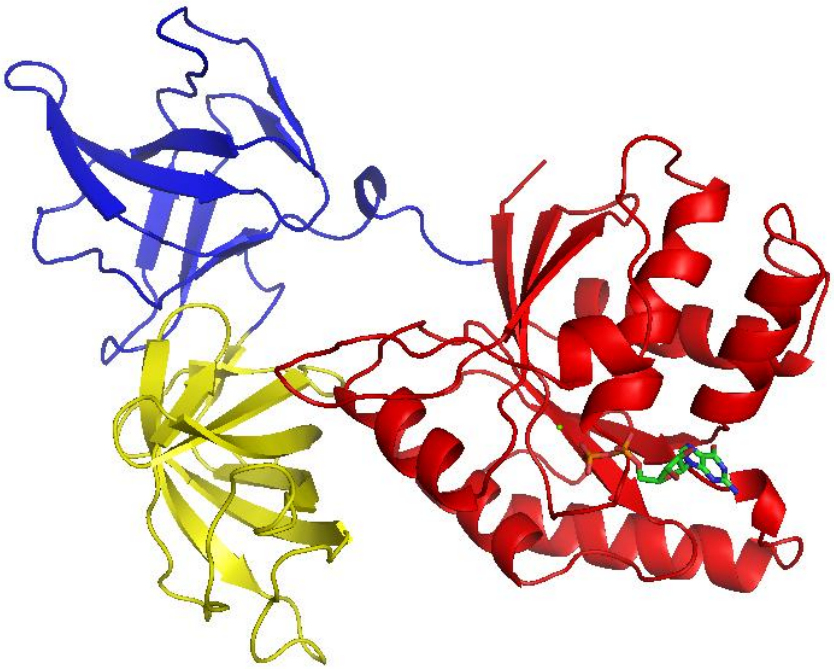

Figure 1.3. Inactive conformation of the EF-Tu·GDP complex (PDB ID: 1TUI).

Domain I consists of 6 β-strands surrounded on both sides by six α-helices in a fold shared by all GBPs. The nucleotide binding pocket has been determined by structural elements containing three GBP consensus motifs (GBP I-III) and two conserved motifs for prokaryotic elongation factors (EF I-II). Switch I and Switch II delimit the guanine nucleotide-binding pocket. In terms of EF-Tu activity, the presence of Mg^{++} ions is essential. Guanine nucleotides always bind to EF-Tu in the presence of Mg^{++} which is bound to the β- and γ- phosphates' oxygen atoms of the GTP or only β- phosphates' oxygen atom of the GDP. Mg^{++} completes its coordination to six. The other two oxygen atoms come from the side chain hydroxyl groups of T62 and T25 which are located in domain I region. The other two oxygen atoms come from two water molecules (Figure 1.4). Domain II and III are only composed of β-strands. These two domains act like a rigid body during the functioning cycle of the EF-Tu [11, 12].

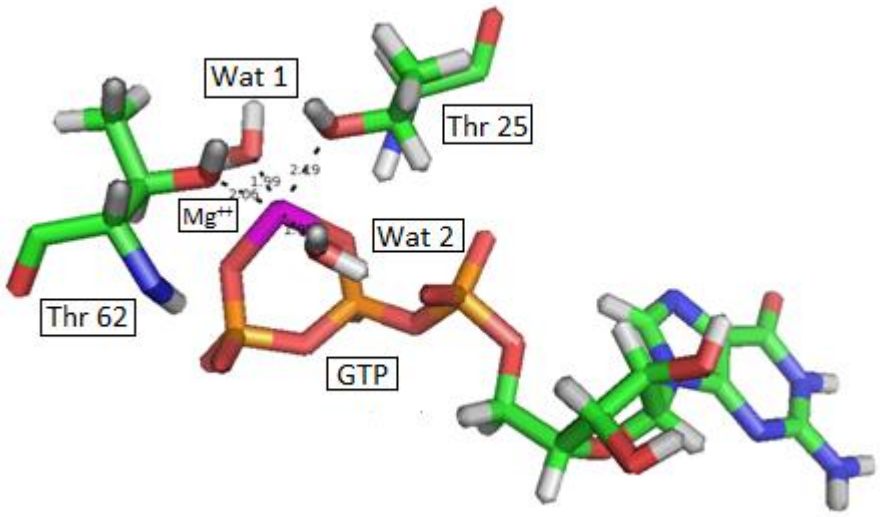

Figure 1.4. Mg^{++} coordination shell (blue: nitrogen atom, green: carbon atom, magenta: magnesium ion, orange: phosphorous atom red: oxygen atom, PDB ID: 1EFT).

EF-Tu has generally two distinct states, an active GTP bound form and an inactive GDP bound form. EF-Tu·GDP form is less compact, and there is very poor interaction between the three domains. However, EF-Tu·GTP is in compact form and has very close interaction between the domains (Figure 1.2 and 1.3).

Closeness of the domains which occurs only in the presence of GTP, leads to a new strong binding site for another macromolecular ligand, aa-tRNA. This new complex, EF-Tu·GTP·aa-tRNA, is called as the ternary complex (Figure 1.5). Strong binding enables the transfer of aa-tRNA to the corresponding site of the ribosome [22]. Moreover, GTP binding to EF-Tu causes another local rearrangement. Switch 1 conformation turns to α-helix from β-strand. This conformational change increases the affinity of EF-Tu to the ribosome. Hence, EF-Tu activity of delivering aa-tRNAs to the corresponding site to the mRNA programmed ribosomes can be sustained in EF-Tu·GTP complex form.

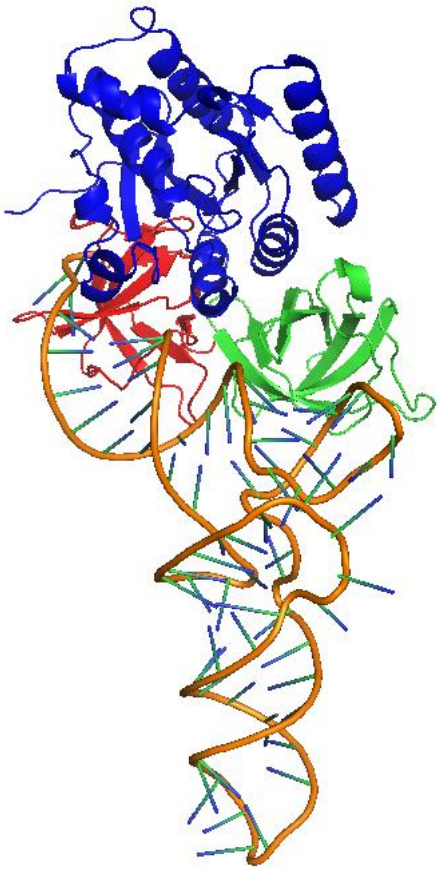

Figure 1.5. Structure of EF-Tu·GTP·aa-tRNA (ternary) complex (PDB ID: 1B23).

Complex structures of EF-Tu·GTP and EF-Tu·GDP show important conformational changes in the Switch 1 and Switch 2 regions. Amino acid sequence of 52^{nd} to 65^{th} residues of EF-Tu is called as the Switch 1 region. This region is composed of two perpendicular α-helices (Figure 1.6).

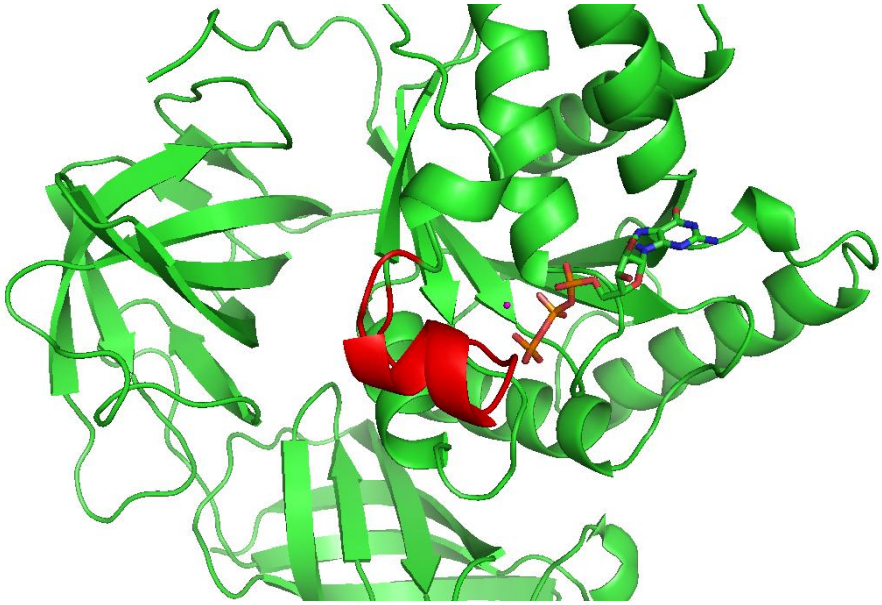

Figure 1.6. Switch 1 region (red) in EF-Tu·GTP complex.

Switch 1 region is part of the aa-tRNA binding site, so its conformation has an extra importance for aa-tRNA binding to EF-Tu. One of these α-helix changes its conformation when GTP is hydrolyzed to GDP and turns into a β-sheet (Figure 1.7).

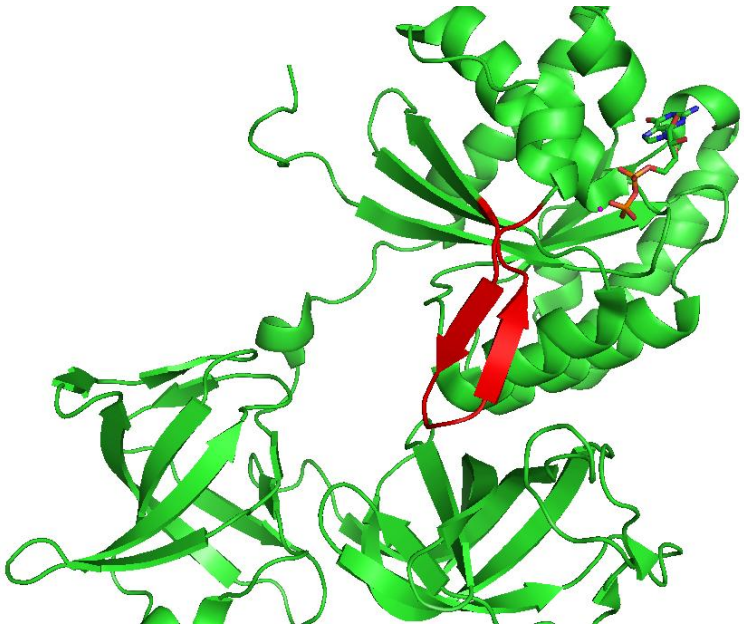

Figure 1.7. Switch 1 region (red) in EF-Tu·GDP complex.

Another conformational change is observed in Switch 2 (aa 82-97) region, going from EF-Tu·GTP to EF-Tu·GDP complex. One α-helical turn unwinds at its C terminus and form new turn at N terminus (Figure 1.8-1.9).

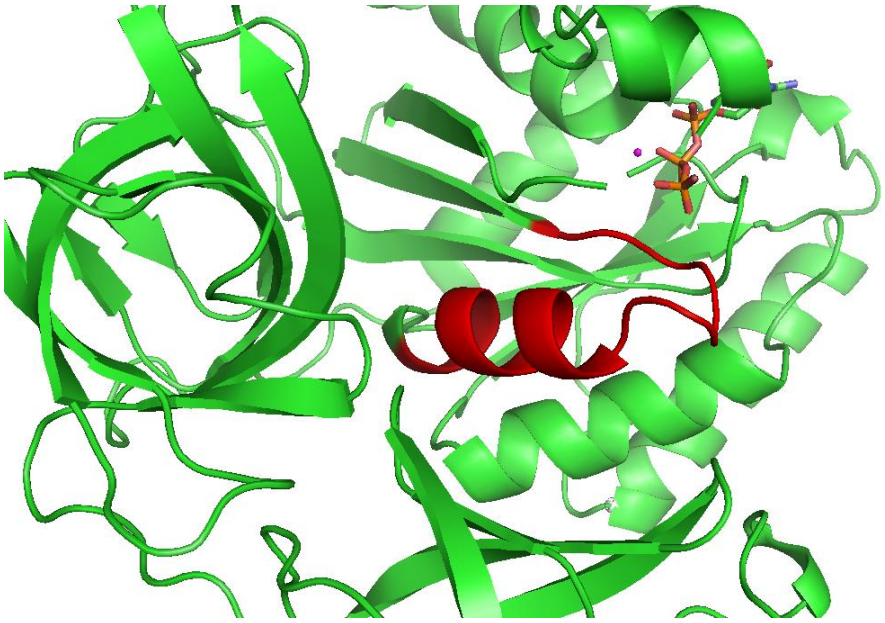

Figure 1.8. Switch 2 region (red) in EF-Tu·GTP conformation.

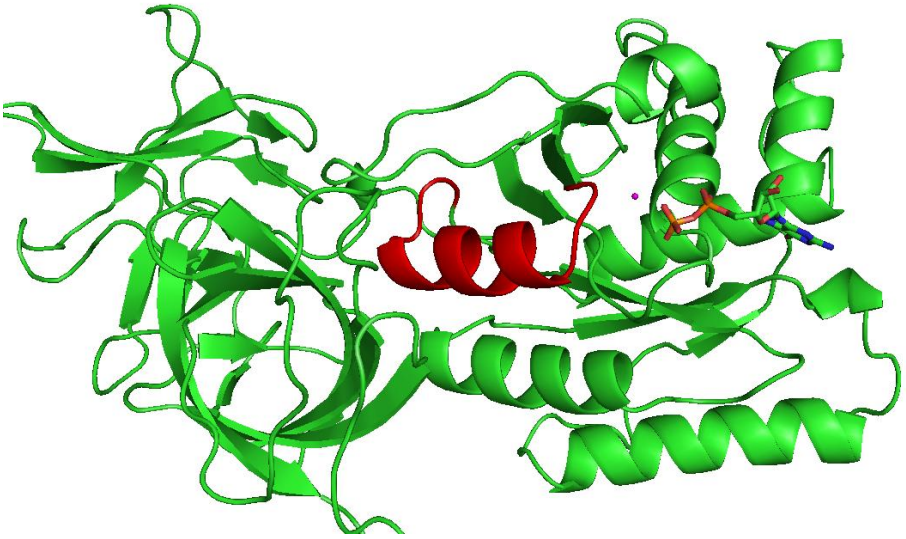

Figure 1.9. Switch 2 region (red) in EF-Tu·GDP conformation.

1.3. Experimental Data on GTPase Activity of Elongation Factor Tu (EF-Tu)

In the last fifteen years, many experimental papers on EF-Tu have been published. Most of these publications aimed to detect both intrinsic and ribosome induced GTPase activity of EF-Tu and affinity of EF-Tu to GTP and GDP by mutating some amino acid residues, especially in the GTP binding pocket. Moreover, in addition to the amino acid residues T25 and T62 which directly coordinate to Mg^{++} ion, D51 and D81 which coordinate to Mg^{++} ion via two water molecules intrigued the researchers most. (Figure 1.10).

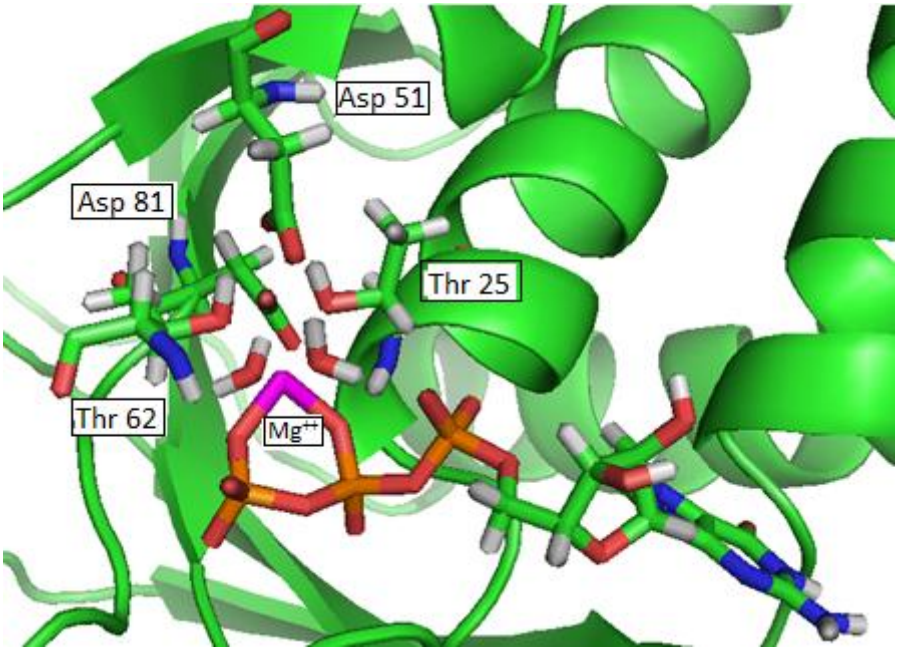

Figure 1.10. Mg^{++} coordination network in EF-Tu·GTP (blue: nitrogen atom, green: carbon atom, magenta: Mg^{++} ion, orange: phosphorous atom red: oxygen atom, PDB ID: 1EFT).

One of the earliest mutational studies is a substitution of T62 which is a part of GTP binding site, to alanine (T62A) and serine (T62S) by using site directed mutagenesis in the EF-Tu from *Thermus thermophilus* [23]. EF-Tu[T62A] shows great decrease in polypeptide synthesis with very low intrinsic and ribosome induced GTPase activity. Dissociation rate of GDP and GTP from EF-Tu are the same with the wild type EF-Tu, which shows that T62 has no contribution to the binding energy. On the other hand, both

intrinsic and ribosome induced EF-Tu[T62S] shows slight decrease in GTPase activity. This result is correlated with increased mobility of the side chain hydroxyl group of serine as compared to the side chain hydroxyl group of threonine. The importance of the methyl group of theronine which is not present in serine, is also supported by the indispensible threonine residue at the homologous position in all G-proteins [24]. These results support the assumption that T62 is in interaction with Mg^{++} ion, γ-phosphate group and one water molecule which is thought to be involved in GTP hydrolysis (Figure 1.11).

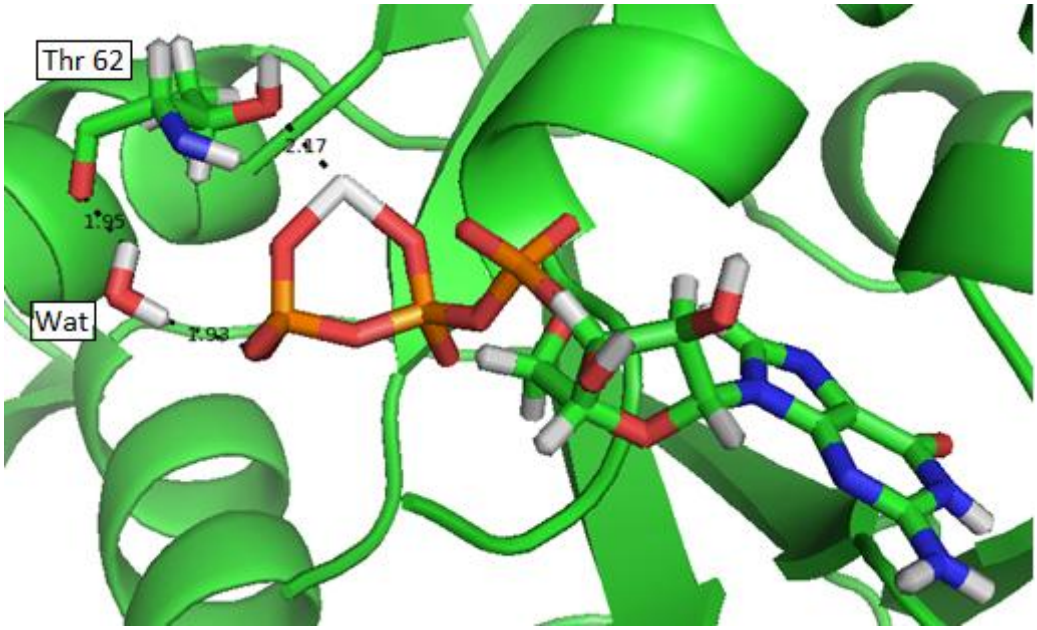

Figure 1.11. T62 in the *T. Aquaticus* EF-Tu·GTP complex, is in interaction with Mg^{++}, hydrolytic water and γ-phosphate group (PDB ID: 1EFT).

There is also comprehensive experimental data about T25 which is another member of Mg^{++} coordination shell. T25 has been mutated to alanine (T25A) and serine (T25S). Nucleotide interaction was moderately destabilized in EF-Tu[T25S] but strongly in EF-Tu[T25A]. EF-Tu[T25S] sustained its function as effectively as in the wild type EF-Tu. Intrinsic GTPase activity of EF-Tu[T25A] showed 90 per cent reduction. T25A mutant formed more stable interaction with EF-Ts than the wild type. This implies that stabilization of EF-Tu·EF-Ts complex is related to the inability to bind Mg^{++}, rather than to a decreased nucleotide affinity [25].

Aspartate 80 (D80) is in the coordination network of Mg^{++} ion and its mutation to an asparagine (D80N) in *Escherichia coli* species [26] or to alanine mutation (D81A) in *Thermus thermophilus* species [27] have been performed (D81 in *T.Aquaticus* species). EF-Tu[D80N] shows less affinity to GDP and binds strongly to EF-Ts. However Asp80 is suggested to have a critical role in GTPase activity, it is stimulated to the same rate as wild type in the presence of empty ribosomes. D80N mutation shows a dramatic change of all interaction parameters. The wild type EF-Tu has several orders higher affinity to GDP than GTP. D80N mutant EF-Tu showed decrease in GDP affinity and it became very close to that of GTP. Aspartate (Asp) has a pKa of 4.4 and mostly ionized, making it an exclusive proton acceptor. In crystal structures, Asp80 is seen to accept H-bond from Thr25 and from one water which is coordinated to Mg^{++}, which donates its other hydrogen toward the Cys82 main chain carbonyl group. An asparagine (Asn) side chain is poorly ionizable and may act both as an H-bond acceptor and donor. Whereas a similar configuration for Asp80 is possible with the Asn amide donating hydrogen to the Mg^{++}-bound water, leaving one amide and one water hydrogen unbounded, the lack of a negative charge attracting the Mg^{++} likely makes the bonding weaker. Impaired Mg^{++} interaction network probably leads to a decrease in intrinsic GTPase activity [26]. Protein degradation is observed when Asp81 in *Thermus thermophilus* is mutated to an alanine (D81A) [27].

EF-Tu and other translation factors have slower intrinsic GTP hydrolysis rate compared with members of the small GTPases, e.g. Ras p21, and heterotrimeric G-proteins, e.g. $G_i\alpha1$ [28]. By the aid of crystal structure data it is known that Gln204 and Arg178 residues stabilize the transition state for the GTPase activity of $G_i\alpha1$ protein. Both transition state stabilizing residues are provided by the protein structure itself. This is why heterotrimeric G-proteins have higher intrinsic GTP hydrolysis rate than small GTPases and much higher than the G proteins in translation. Specific GAPs can increase the hydrolysis rate of heterotrimeric G-proteins. Lower activity in small GTPases like Ras p21 proteins, can be explained by the absence of arginine residue that is homologous to the one in the heterortrimeric G-protein [28]. This is in good agreement with their biological function because of biological signal requirement for the GTP hydrolysis. Crystal structure of Ras p21 with specific RasGAP provides the presence of important ‘Arg finger’ residue as a transition-state-stabilizing side chain, in a similar position of Arg178 in $G_i\alpha1$. Ras p21 itself also provides Gln61 to stabilize the transition state (Figure 1.12). Substrate-assisted

GTP hydrolysis mechanism is thought for Ras p21, and in this model, γ-phosphate group oxygen of GTP acts as a base that abstracts a proton from the catalytic water and the newly formed hydroxyl group can act as a better nucleophile during the hydrolysis [19, 28].

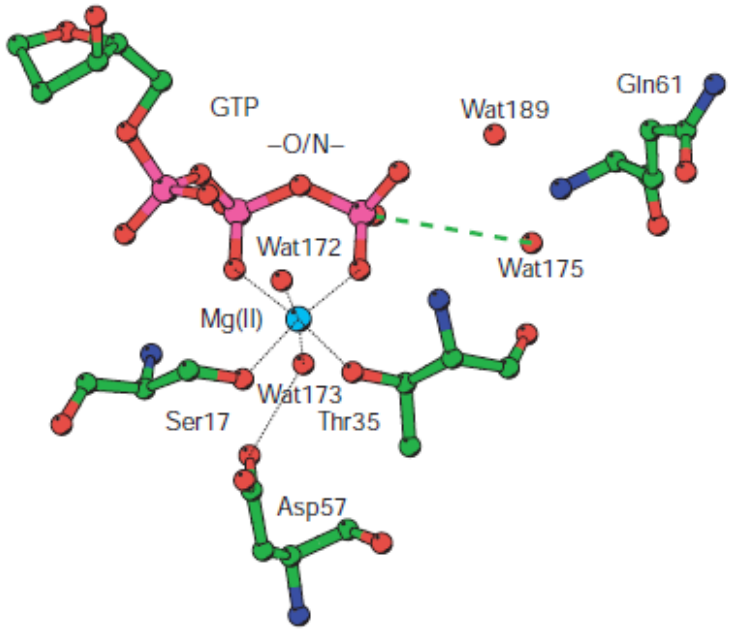

Figure 1.12. The active site of p21Ras in complex with GTP and the catalytic mechanism for the intrinsic hydrolysis [28].

After these observations, researches concentrated on the lower intrinsic GTPase activity of translation factors than other members of G-protein families. His84 in switch 2 of *E.coli* and His 85 of *T. aquaticus* and *T. thermophilus* have been suggested as functional homologous to Gln204 of $G_i\alpha 1$ and Gln61 of Ras p21 [29]. Furthermore, Arg59 from *T. aquaticus* and *T. thermophilus* (Arg58 of *E.coli*) in the Switch 1 region is in a sequence environment similar to that of Arg178 in Giα1. Both arginine residues are close to a threonine residue, which is known to provide a ligand to the Mg^{++} ion in the GTP form. Arg59 was mutated to alanine in *E.coli* (R58A) and to glutamic acid (R58E) to investigate the role of this residue in GTP hydrolysis and binding of aa-tRNA to the EF-Tu. Intrinsic GTPase activity of R58A and R58E mutants showed the same GTPase activity as the wild type protein, but a large reduction in the ribosome induced hydrolysis was observed. Use of high ribosome concentrations brings the hydrolysis rate to the same level as the wild type [30]. These results indicate that R58 may not have a catalytic role in ribosome

induced hydrolysis but it is probably involved in the binding of EF-Tu to ribosome. R58 mutations did not change the affinity of EF-Tu to the guanine nucleotides but it was also found that R58 was involved in binding of aa-tRNA to the EF-Tu [29, 30].

Binding of the antibiotic kirromycin to EF-Tu stimulates its intrinsic GTPase activity. His85 in some crystal structures is seen out of the catalytic site which is in the very similar position of the kirromycin bound ternary complex of EF-Tu. On the other hand, crystal structure of aurodox, which is another GTPase activating antibiotic, bound to EF-Tu·GDP shows that His85 is in a very close position to the nucleotide binding site than other known structures of EF-Tu. All these findings demonstrate that His85 can be brought into a position where it may play a crucial role in GTP hydrolysis [31].

In one experimental study, Parmeggiani et. al. mutated histidine 84 to the alanine (H84A) and glutamine (H84Q), in *E.coli* EF-Tu [32]. Binding of GTP and GDP is slightly affected by these mutations. H84Q displays 35 per cent activity as compared to the wild type protein in polypeptide synthesis and GTP hydrolysis. However, H84A has no intrinsic activity in polypeptide synthesis but 10 per cent residual GTPase activity. On the other hand, kinetic studies on H84A mutant showed that only GTP hydrolysis step decreased sharply, other elemental steps in polypeptide synthesis were not affected very much [32]. Ribosome can induce the GTPase activity of EF-Tu H84Q mutant but not that of EF-Tu H84A. In terms of H84Q mutation, GTP hydrolysis rate is moderately reduced when ternary complex binds to the programmed ribosome. Effect of mRNA programmed ribosome to the ternary complex, EF-Tu·GTP·aa-tRNA, may lead to dramatic conformational change of the factor(s) which can enable to activate a water molecule as a nucleophile, this factor may be H84. These results may indicate that, H84 has a catalytic role on the ribosome induced GTPase activity but does not have a crucial role in intrinsic activity [32].

A GTP hydrolysis mechanism in which His85 has an active role is suggested. By analogy to other GTP-binding proteins, the reaction is likely to proceed by a direct in-line attack of a water molecule on the γ-phosphorus atom of GTP. In earlier studies of Ras-like proteins, Gln residue has been thought as the catalytic residue. Gln would abstract a proton from attacking water and newly formed hydroxide ion would act as a better nucleophile.

However, both experimental and theoretical analysis explained that pKa of the Gln residue is too low for a general-base function [33]. Similar approach has been developed for His 85 of EF-Tu by Nemukhin et. al. in a theoretical study [34]. They assumed that His 85 would act as a general base and investigated energy barriers of GTP hydrolysis in EF-Tu by locating His 85 in ($His85_{in}$) and out ($His85_{out}$) of the active site (Figure 1.13-1.16).

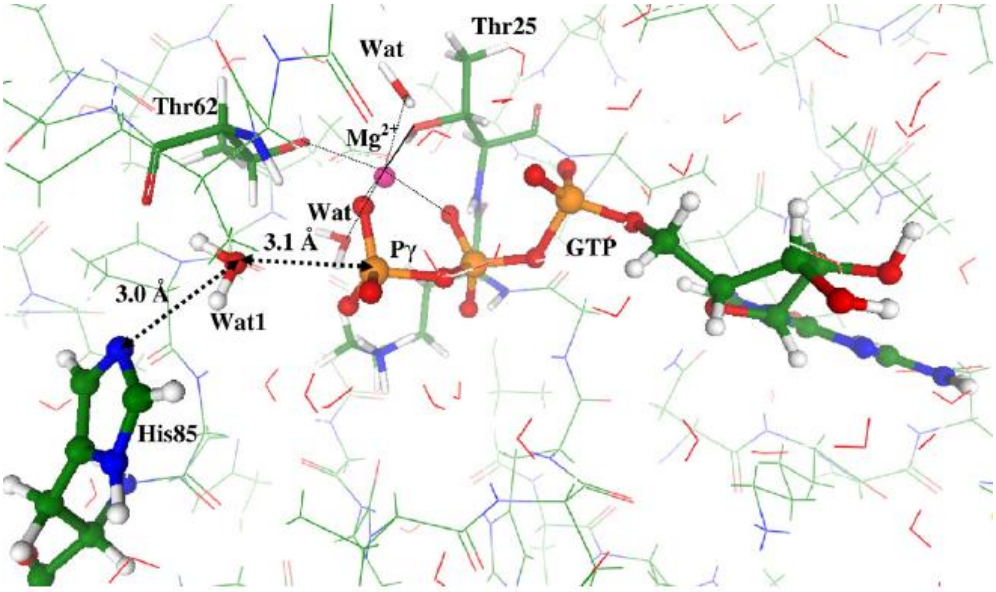

Figure 1.13. Geometry of $His85_{in}$ model, before the transition state [34].

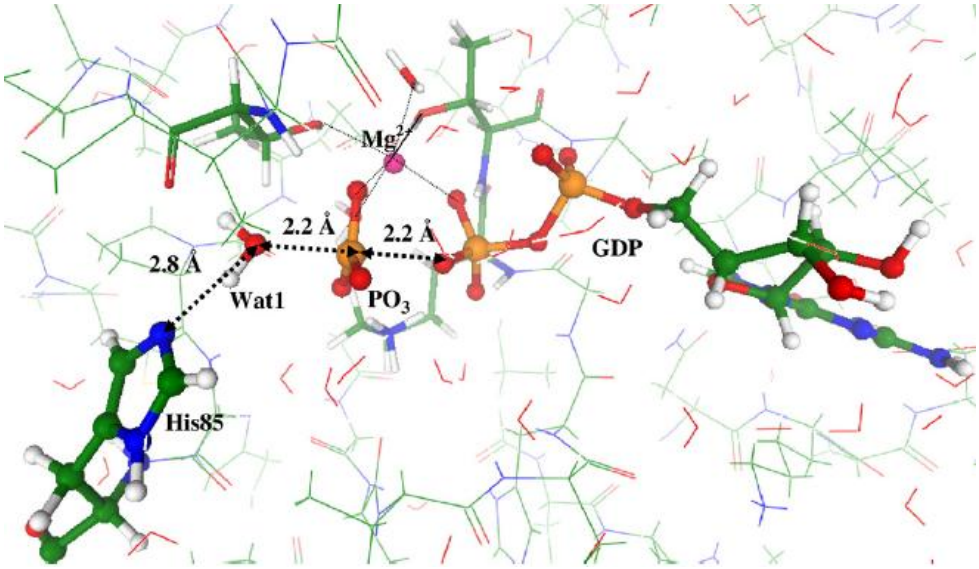

Figure 1.14. Transition state geometry of $His85_{in}$ model [34].

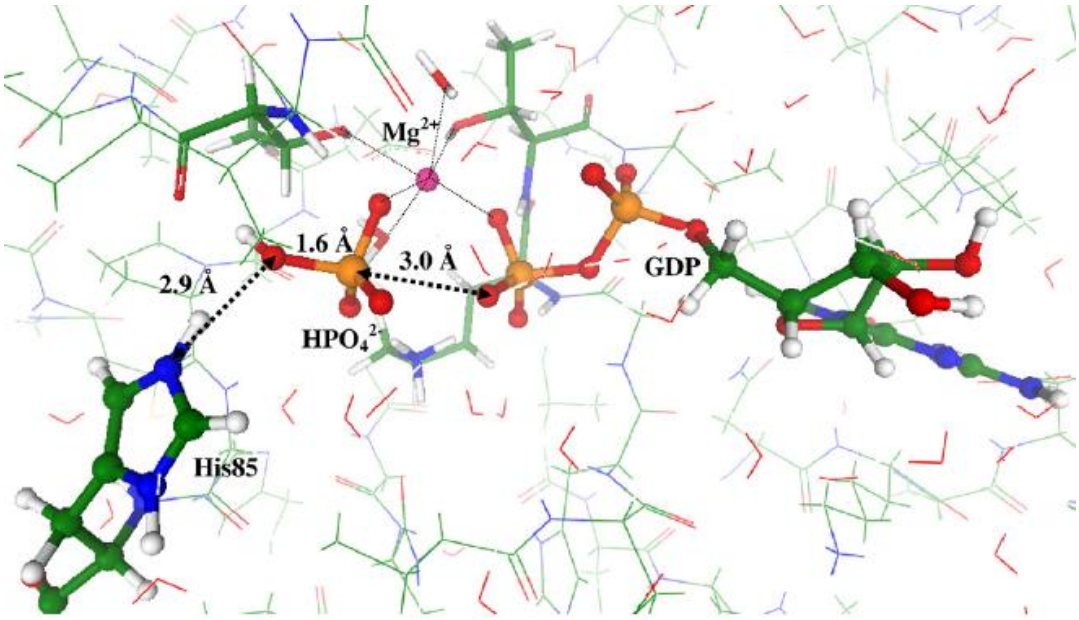

Figure 1.15. Geometry of $His85_{in}$ model, after the hydrolysis [34].

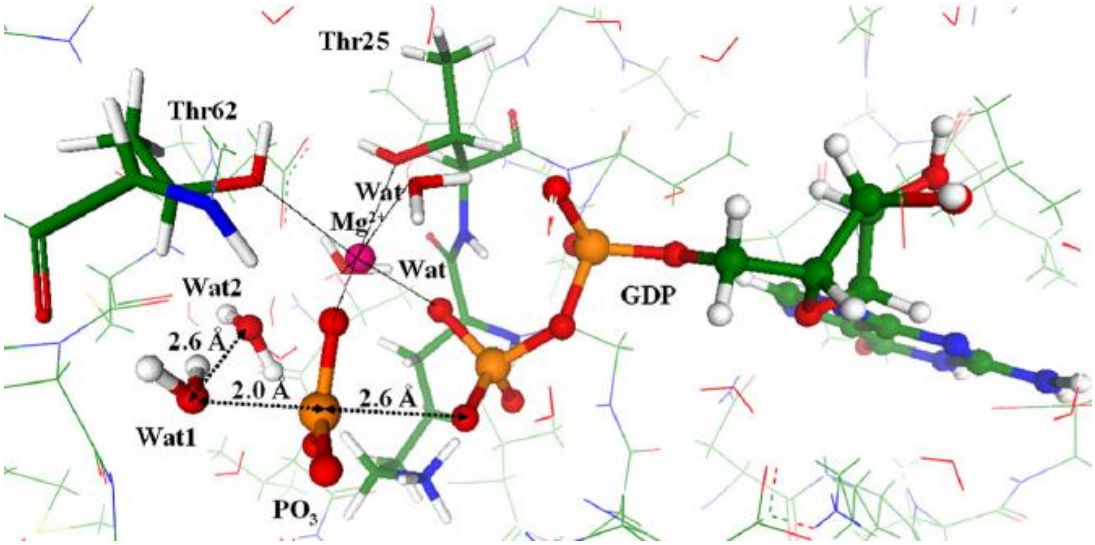

Figure 1.16. Transition state geometry of $His85_{out}$ model [34].

When His85 residue is out of the catalytic site, extra water molecule assist the hydrolysis and after including all entropic contributions, GTP hydrolysis activation barrier is calculated as 10.7 kcal/mol and 21.3 kcal/mol for $His85_{in}$ and $His85_{out}$ models,

respectively. These results support that His85 eases the GTP hydrolysis but requires additional factors, i.e. presence of programmed ribosomes, to be placed near the active site [34].

Crystal structures of several Ras-like and heterotrimeric G proteins indicated that the Gln residue stabilizes the GTPase transition state by positioning both water molecule and γ-phosphate. As far as His85 of EF-Tu is concerned it may act similar to conserved Gln in switch II region of Ras-like proteins. pH dependency of GTPase activation and GTPγS hydrolysis are studied to examine the general base mechanism of His85 which is thought to abstract a proton from attacking water molecule. No pH dependence is observed which excludes the general base role of His85 in GTP hydrolysis [35].

The most realistic role of His85 similar with Gln61 in Ras-like proteins is that, it stabilizes the GTPase transition state by dictating the hydrolytic water and γ-phosphate group (Figure 1.17).

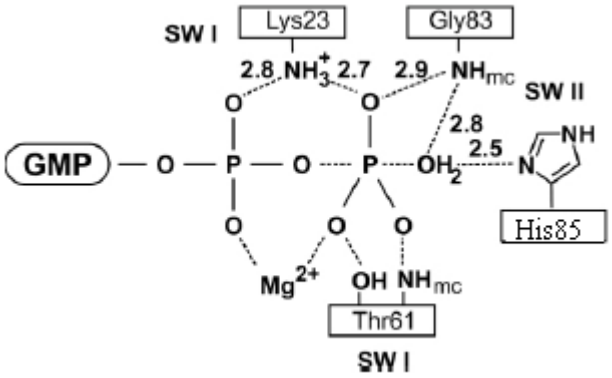

Figure 1.17. His85 positioning the hydrolytic water [35].

Related to His85 activity, there are two other important residues in EF-Tu: valine 20 (V20) and isoleucine 60 (I60). In structures of EF-Tu·GTP complex, His85 points away from the catalytic site and its access to the GTP and hydrolytic water molecule is hindered by the side chains of Val20 and Ile60 that form a hydrophobic gate (Figure 1.18). It was proposed that, in order to accelerate the GTP hydrolysis, one or both wings of the hydrophobic gate could open, providing access of His85 to the γ-phosphate [36]. However,

neither mutation valine to glycine (V20G) nor isoleucine to alanine (I60A) increased the GTPase activity [26, 37].

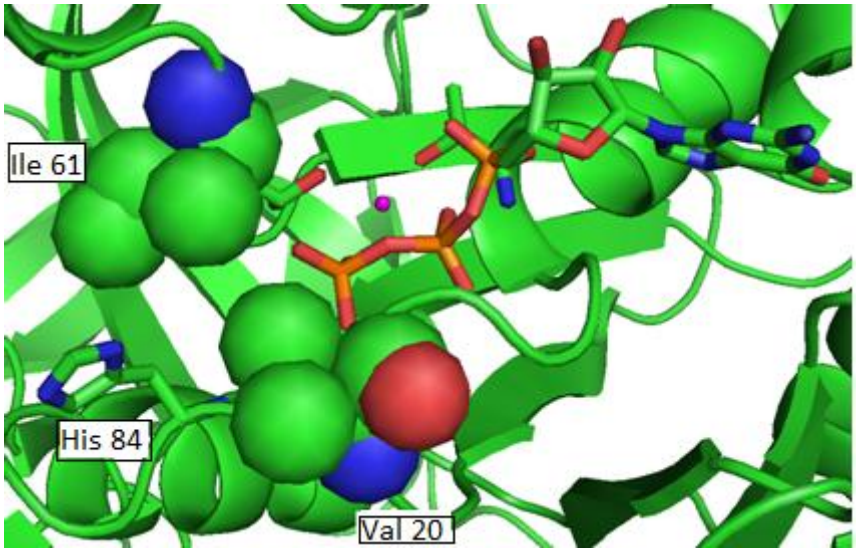

Figure 1.18. Position of His84 and hydrophobic gate. Ile61 and Val20 are shown with spheres (PDB ID: 1EFT).

2. AIM OF THE STUDY

The purpose of this study is to investigate the role of important amino acids in GTPase activity of EF-Tu·GTP complex from *Thermus aquaticus* by aid of molecular dynamic simulations. The study has been carried by comparing the experimental results with the results of the MD simulations.

3. METHODOLOGY

Molecular Dynamics (MD) simulations can be applied in the investigation of a wide range of dynamic properties and processes by researchers in numerous fields, including structural biochemistry, biophysics, enzymology, molecular biology, pharmaceutical chemistry, and biotechnology. Simulations can provide the ultimate detail concerning individual particle motions as a function of time. Thus, they can be used to address specific questions about the properties of a model system, i.e. specific aspects of biomolecules, kinetics and thermodynamics, often more easily than experiments on the actual system. Furthermore a variety of studies including drug design and protein design, structural determination and refinement can be performed via MD. Experiments play essential role in validating the simulation methodology: comparisons of simulation and experimental data serve to test the accuracy of the calculated results and to provide criteria for improving the methodology [38].

Recently, molecular dynamics simulations have been widely used to test the structure, dynamics and thermodynamics of biological molecules as well as for the determination of structures from X-ray crystallography and from NMR experiments.

3.1. Force Fields

In the context of molecular mechanics, a force field refers to the functional form and parameter sets used to describe the potential energy of a system of particles (typically but not necessarily atoms). Force field functions and parameter sets are derived from both experimental work and high-level quantum mechanical calculations. A force field is mainly composed of two parts: bonded terms and non-bonded terms. Bond stretching, angle bending and torsion angle can be taken into bonded terms, similarly, van der Waals and Coulomb forces can be taken into non-bonded terms contributions (Figure 3.1).

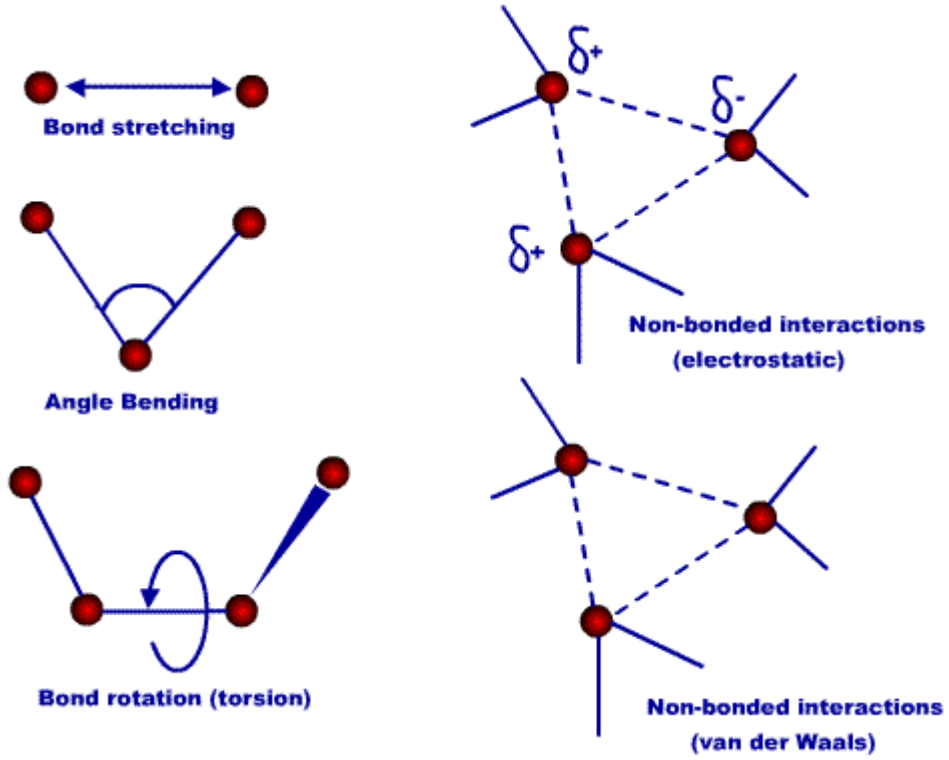

Figure 3.1. Force field contributors.

By using these contributions to the potential energy, E, can be evaluated as the following:

$$E = E_b + E_s + E_\omega + E_{nb} \tag{3.1}$$

E_s is the energy for bond stretching, E_b is the energy for bond angle bending, E_ω is the torsional energy due to twisting about bonds and E_{nb} is the energy for non-bonded interactions. Many different kinds of force-fields have been developed over the years. Some include additional energy terms that describe other kinds of deformations. Some force-fields account for coupling between bending and stretching in adjacent bonds in order to improve the accuracy of the mechanical model.

The design of force-fields for molecular mechanics is guided by the following principles:

i) Nuclei and electrons are lumped into atom-like particles.

ii) Atom-like particles are spherical (radii obtained from measurements or theory) and have a partial charge (obtained from theory).

iii) Interactions are based on springs and classical potentials.

iv) Interactions parameters must be preassigned to specific sets of atoms types.

v) Interactions determine the spatial distribution of atom-like particles and their energies.

3.1.1. Stretching and Bending

Considering the idea of a molecule to be a collection of masses connected by springs, by applying Hooke's Law we can evaluate the energy required to stretch and bend bonds from their ideal values. Thus E_s and E_b may be expressed as:

$$E_s = \sum_{i=1}^{N} \frac{k_i^s}{2} (l - l_0)^2 \tag{3.2}$$

$$E_b = \sum_{i}^{M} \frac{k_i^b}{2} (\theta - \theta_0)^2 \tag{3.3}$$

where N is the total number of bonds and M is the total number of bond angles in the molecule. k^s and k^b are the force constants for stretching and bending respectively. l and θ are the actual bond lengths and bond angles. Finally l_0 and θ_0 are ideal bond lengths and bond angles. Unique k^s and l_0 values are assigned to each pair of bonded atoms based on their types (e.g. C-C, C-H, O-C, etc.). Similarly k^b and θ_0 parameters for angle bending are assigned to each bonded triplet of atoms based on their types (e.g. C-C-C, C-O-C, C-C-H, etc.).

3.1.2. Torsion

We consider the form of the E_ω term. The energy due to torsion is usually expressed in terms of a Fourier series,

$$E_\omega = \sum \frac{V_n}{2} (1 + \cos[n\emptyset - \gamma]) \tag{3.4}$$

where the sum is over all unique sequences of bonded atoms. ω is the torsion angle and γ is the phase factor.

3.1.3. Non-Bonded Interactions

The final term contributing to E is the energy from pairwise non-bonded interactions. These interactions are van der Waals forces and electrostatic interactions.

$$E_{non-bonded} = \underbrace{\sum_i \sum_{j>i} \left(\frac{A_{ij}}{r_{ij}^{12}} - \frac{B_{ij}}{r_{ij}^{6}} \right)}_{van\ der\ Waals} + \underbrace{\sum_i \sum_{j>i} \frac{q_i q_j}{\varepsilon r_{ij}}}_{Coulomb} \tag{3.5}$$

where, van der Waals interaction between two atoms i and j separated by distance r_{ij} is described by Lenard Jones potential with parameters A_{ij} and B_{ij}, and a Coulomb potential describes the electrostatic interaction between a pair of atoms i and j using q_i and q_j as partial charges on the atoms and ε as the dielectric constant of medium.

Usually the parameters for the non-bonded energy terms are obtained by measuring non-bonded contact distances in crystalline hydrocarbons, diamond, graphite and van der Waals contact data for rare gas atoms. Parameters for other atoms are then obtained by extrapolation or interpolation. One major assumption is that the potential derived from intermolecular interactions can accurately reproduce intramolecular interactions. In addition the interactions are considered to be pairwise additive [39].

An important non-bonded energy term that is always taken into account is the electrostatic interactions. Typically the electrostatic interaction dominates the total energy

of a system by a full magnitude. The electrostatic contribution is modeled using a Coulombic potential.

The electrostatic energy is a function of the charge on the non-bonded atoms, their interatomic distance, and a molecular dielectric expression that accounts for the decrease of electrostatic interaction due to the environment (such as by solvent or the molecule itself). A linearly varying distance-dependent dielectric (i.e. 1=r) is sometimes used to account for the increase of ε in environmental bulk as the separation distance between interacting atoms increases. The accuracy of the electrostatic term depends on the correct assignment of charges to individual atoms.

The terms describing energy changes from bond length, bond angle and torsions are well understood and can be accurately included in the overall energy expression. The most influential term, the electrostatic term, however is not fully understood. Hence the variation in results from different force fields can be attributed, to a large extent, to the electrostatic term. Of course the nature of the parameterizations generating the various force constants and ideal lengths and angles will also affect the applicability of a force field. In general one must consider with which group of molecules or systems a given force field has been parameterized – keeping this fact in mind one may then use the force field on an unknown but similar system. Generality is still a problem with force fields, though with the development of the Universal Force Field (UFF) [40] an attempt has been made to develop a generalized force field applicable to a large portion of the periodic table and not be restricted to particular groupings of atoms such as proteins, nucleic acids etc.

3.2. Theory of Molecular Dynamics

The state of any classical system can be completely described by means of specifying the positions and momentum of all particles:

$$\mathbf{q} = (x_1, y_1, z_1, x_2, y_2, z2, \ldots)$$
$$p = (p_{x,1}, p_{y,1}, p_{z,1}, p_{x,2}, p_{y,2}, p_{z,2}, \ldots) \quad (3.6)$$

Since a phase point is defined by the positions and momentum of all particles, it determines the location of the next phase point in the absence of outside forces acting upon the system. Therefore, the relationship between two positions in any time interval is given by:

$$\mathbf{q}(t_2) = \mathbf{q}(t_1) + \int_{t_1}^{t_2} \frac{p(t)}{m} dt \tag{3.7}$$

where;

$$v = \frac{p}{m} \tag{3.8}$$

Similarly, the relationship between any two momentum vectors is:

$$p(t_2) = p(t_1) + m \int_{t_1}^{t_2} a(t) dt \tag{3.9}$$

using Newton's Second Law of Motion:

$$a = \frac{F}{m} \tag{3.10}$$

Moreover, the average value of any property during this time evolution is:

$$\langle A \rangle = \frac{1}{M} \sum_i^B A(t_i) \tag{3.11}$$

where B is the number of times the property is sampled. Sampling continuously and following the trajectory indefinitely, this equation becomes:

$$\langle A \rangle = \lim_{t \to \infty} \frac{1}{t} \int_{t_0}^{t_0 + t} A(t) dt \tag{3.12}$$

assuming ergodic hypothesis to be valid and independent of choice of t_0 [41].

3.3. Simulation Parameters

To perform a Molecular Dynamics simulation an initial configuration of the system at the initial time, t=0, and initial velocities of atoms are required. EF-Tu·GTP conformation of *Thermus aquaticus* and *Escherichia coli* of which PDB IDs are 1EFT and 1OB2, respectively, are obtained from Brookhaven Protein Data Bank [19] to be used as the starting point of the MD simulations. Maxwell-Boltzmann distribution assigns the initial velocities, atom i with mass m_i has a velocity v_x in the x-direction at temperature T. These velocities are adjusted so that the total momentum of the system is zero. To set the total linear momentum of the system to zero, the sum of the components of the atomic momentum along the x, y and z axes is calculated. Thus, total momentum of the system in each direction is calculated, and then this value is divided to the total mass and subtracted from the atomic velocities to give an overall momentum of zero.

$$p(v_{ix}) = \left(\frac{m_i}{2\pi k_b T}\right)^{\frac{1}{2}} \exp\left[-\frac{1}{2}\frac{m_i v_{ix}^2}{k_b T}\right] \tag{3.13}$$

$$p = \sum_{i=1}^{D} m_i v_i = 0 \tag{3.14}$$

In a system, temperature and velocities are connected through the following equation:

$$T = \frac{2}{3Nk_b}\sum_{i=1}^{D}\frac{1}{2}m_i\langle v_i^2\rangle \tag{3.15}$$

where k_b is the Boltzmann constant, D is the number of atoms in the system, $\langle v_i^2\rangle$ is the squared velocity of ith atom [42].

AMBER 10 [43] simulation package with ff03 [44] and ff99SB [45] force fields have been used by introducing GTP parameters into the system [46]. The protein has been solvated explicitly in a truncated octahedron box by using TIP3P type water parameters [47]. 12 Na^+ ions have been added to neutralize the medium (The amount of metal ions introduced to the system depends on the protonation state of the protein).

After the system has been prepared, a minimization has been done to get rid of undesired steric clashes and relaxing bond lengths and bond angles which are distorted from their respective minima. In a minimization procedure, given a set of *N* independent variables, *r*, where $r = (r_1, r_2, r_3, \ldots, r_N)$, a set of values r_{min}, for which a function, *E(r)*, has a local minimum, is searched. In terms of a molecular mechanics protein system, *N* is three times the number atoms (three degrees of freedom for each atomic coordinates). *E* is the potential energy provided by the equation 3.1. For a minimization task, there are two widely used methods by utilizing first order derivatives (steepest descent and conjugate gradient), and second order derivatives (Newton-Raphson method).

The steepest descent method is one of the several first-order iterative descent methods. This method uses the gradient of the potential-energy surface, which directly relates to forces in the MM description of molecular systems, to bring the system towards the nearest local energy minimum. In an iterative descent method, for iteration *k*, the next configuration is determined by applying the relationship $x(k) = x(k-1) + \lambda(k)F(k)$, where *x* is the position vector in 3N dimensional space, $\lambda(k)$ is a step size, and F(k) is the force vector. Step size is arbitrary for the first step; however, after every iteration this step size is adjusted according to whether the overall potential energy of the system was reduced or increased by that step. This adjustment keeps the step size almost appropriate for the particular curvature of the potential-energy function in the region of interest. Steepest descent method is very useful in removing steric clashes and relaxing bond angles and bond lengths to their canonical values, and locating closest minima, however, highly inefficient for multidimensional problems with irregular potential surfaces [48]. The conjugate gradient algorithm includes two basic steps: adding an orthogonal vector to the direction of research, and then move them in another direction nearly perpendicular to this vector. These two steps are as well known as: step on the valley floor and then jump down.

In our study we used both, steepest descent and conjugate gradient methods for minimization. It is started with steepest descent method to approach a local minimum quickly. And then conjugate gradient method is used to be able to locate the minimum energy point elegantly. After minimizations, simulations have been carried out. Since the initial velocities are arbitrary, starting at the simulations at temperatures around 300-350 K

would yield high arbitrary initial velocities and would result in instabilities. Hence, simulations have been started at 10^0 K. Then, the systems have been heated by using Langevin thermostat for 500ps, from 10^0 K to the 343^0 K and 310^0 K for *Thermus aquaticus* and *Escherichia coli*, respectively, i.e. temperature they thrive. Then the temperature is maintained by a Berendsen thermostat. A Berendsen thermostat is a proportional type of thermostat, and corrects deviations of T from the set point T_0 by multiplying the velocities by a factor to control the value of T [49]. The Langevin thermostats follow the Langevin equation of motion instead of Newton's equation of motion. In the Langevin equation of motion, a frictional force added to the conservative force is proportional to the velocity, and it adjusts the kinetic energy of the particle so that the temperature matches the set temperature.

$$ma = -\zeta v + f(r) + f' \tag{3.16}$$

m is mass of a particle, a is acceleration, f(r) is conservative force acting on the particle, v is the velocity of the particle, ζ is a frictional constant, and f′ is a random force. The frictional force $-\zeta v$ decreases the temperature because ζ is a fixed positive value. The random force is randomly determined from a Gaussian distribution to add kinetic energy to the particle, and its variance is the function of set temperature and time step. Therefore, the random force is balanced with the frictional force and maintains the system temperature at the set value [50]. The pressure is maintained at 1 bar using a non isotropic weak coupling algorithm.

All hydrogen containing bonds are constrained by applying the SHAKE algorithm [51]. Constrain application in biomolecular systems is a very common tradition. It supplies three main advantages. First, the fastest motion frequency determines the maximal integration time step of the system. The highest frequencies are generally related with hydrogen containing bond vibrations. Constraining bond lengths involving hydrogen allows an increase in the simulation time step, and thus a decrease in computational cost to get a trajectory in a desired length. Second, when the range of motional frequencies in a molecular system is very broad, the exchange of energy between the high- and low-frequency modes may be slow. Differences in the accuracy of the forces computed for different modes may result in different heating rates, and, when the heat exchange is slow,

different effective temperatures. Bond-length constraints almost overcome this problem by narrowing the range of frequencies in the system. Third, if the vibrational frequency of a mode is larger than k_bT/h, where k_b is Boltzmann's constant, T the absolute temperature, andhydrogenPlanck's constant, the vibration must be treated quantum mechanically. At room temperature, this is the case for most bond-stretching frequencies. In this case, treating bonds as constraints is probably a better approximation of their quantum-mechanical behavior than treating them as classical harmonic oscillators [52].

All simulations have been performed under periodic boundary conditions. We run our simulations to predict and study the properties of a system in bulk and we are not interested in surface effects. Because of computational resource limitations, our simulations track only a small number of particles to save time. As a result, most molecules are near the edge of the sample, that is near its ``surface." Therefore, we cannot avoid surface effects in our calculations. The system size would have to be extremely large to ensure that the surface has only a small influence on the bulk properties, but this system would be too large to simulate. Surface effects can be ignored for all system sizes when periodic boundary conditions are applied. In periodic boundary conditions, a truncated octahedron simulation box is replicated throughout space to form an infinite lattice. In the course of the simulation, when a molecule moves in the central box, its periodic image in every one of the other boxes moves with exactly the same orientation in exactly the same way. Thus, as a molecule leaves the central box, one of its images will enter through the opposite face. There are no walls at the boundary of the central box, and the system has no surface. The central box simply forms a convenient coordinate system for measuring locations of the N molecules. A two-dimensional version of such a periodic system is shown in Figure 3.2. As a particle moves through a boundary, all its corresponding images move across their corresponding boundaries. The number of particles in the central box (and hence in the entire system) is conserved.

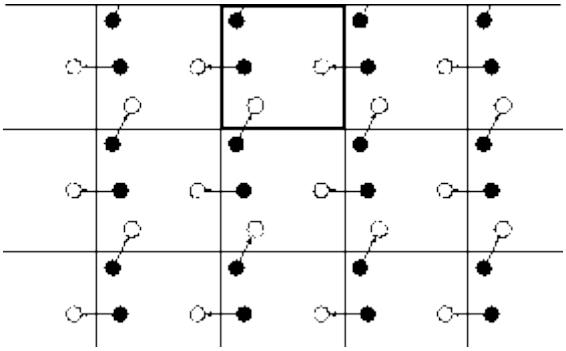

Figure 3.2. Periodic boundary conditions (The central box is outlined by a thicker line).

A cut off distance 9 Å has been used for calculating Lenard-Jones potential and electrostatic interactions. The Particle Mesh Ewald method has been used in calculating the electrostatic interactions. 15 different simulations have been performed with Particle Mesh Ewald Molecular Dynamics (PMEMD) up to 15-30ns with a time step of 2fs by recording coordinates at each 200 steps.

4. RESULTS AND DISCUSSION

4.1. Validation of Simulations

In our study we performed twelve simulations that have been carried out using the ff03 force field. Out of these 12 simulations, three simulations have been performed on the wild type *Thermus aquaticus* (PDB ID: 1EFT) with three different protonation states of H85 (Figure 4.1). An additional simulation with a larger solvent box has been used to make sure that the smaller box size used in the other simulations is appropriate. A fifth simulation has been done on the wild type Escherichia coli (PDB ID: 1OB2) species with H84 protonated.

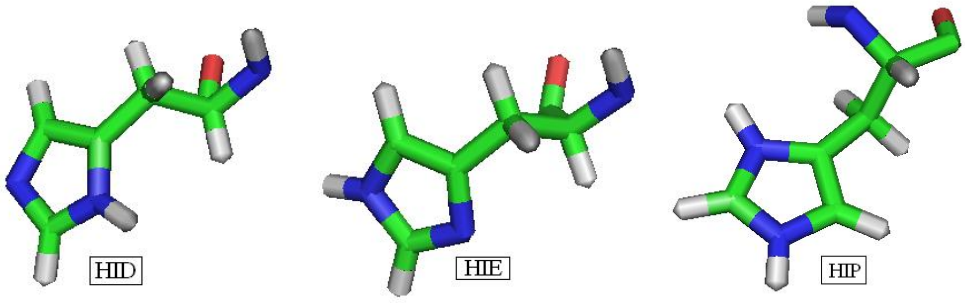

Figure 4.1. Different protonation states of histidine residue.

We have simulated different mutant *Thermus Aquaticus* EF-Tu structures in order to understand and explain the available experimental data in a more detailed way. In addition, two simulations have been carried out using the ff99SB force field and compared with the ff03 data in order to make sure that the results presented in the following sections are not an artifact of the ff03 force field. All performed simulations are listed in Table 4.1.

Table 4.1. MD simulations.

	MD SIMULATIONS			
	FF03		FF99SB	
Thermus Aquaticus	D87EI61A	15 ns	H85HID (wt)	20 ns
	D87EHIP85	20 ns	H85HIP (wt)	20 ns
	H85A	20 ns		
	D21P	25 ns		
	R57A	15 ns		
	R57Rb	8 ns		
	T62A	10 ns		
	H85HID (wt)	30 ns		
	H85HIE (wt)	20 ns		
	H85HIP (wt)	30 ns		
	H85HIP (wt) [20Å water]	10 ns		
E.coli	H85HID (wt)	30 ns		

Before analyzing the dynamical features of the individual components of the protein, a root mean square deviation (RMSD) calculation, temperature (T) and density (d) evaluations have been done to make sure that simulation reached to a convergence point. All simulations have shown the same temperature and density graphs. On the other hand, *Escherichia coli* thrive at 310^0K so its Temperature-time graph is different than the *Thermus aquaticus'* ones (Figure 4.2, 4.3). (Temperature and density values of first 5ns EF-Tu[H85(HIP)] simulation were supplied as a representative.)

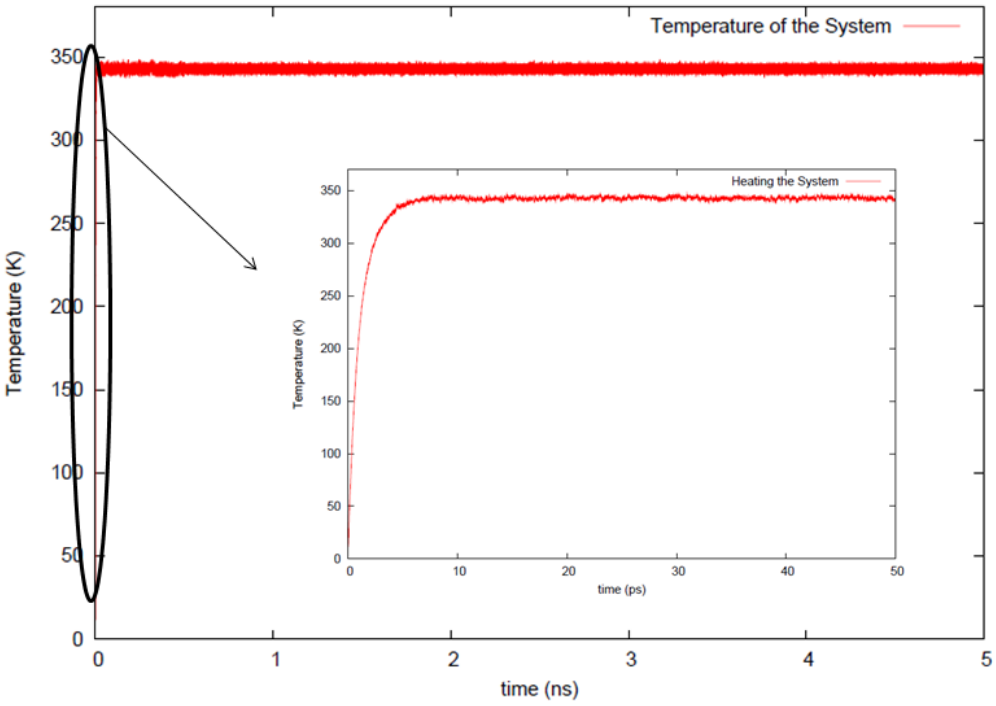

Figure 4.2. Temperature values of wild type EF-Tu[H85(HIP)] simulation.

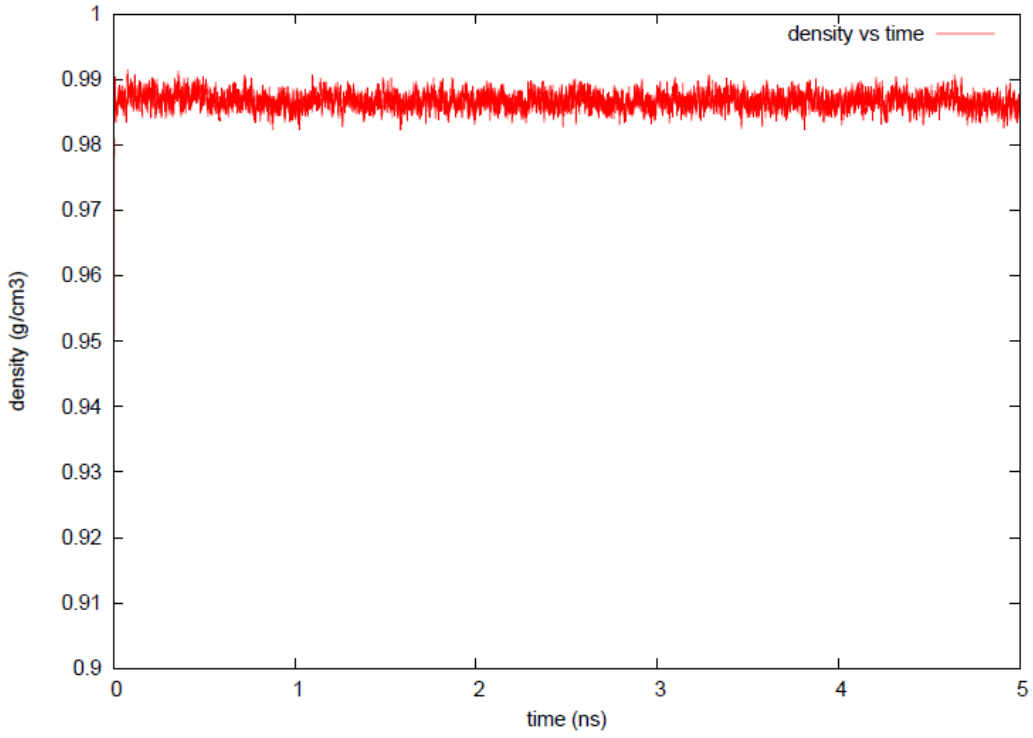

Figure 4.3. Density values of wild type EF-Tu[H85(HIP)] simulation.

C_α atoms of amino acid residues except for first eight residues which are very dynamic and have no functional property during the EF-Tu activity are used to extract RMSD values. Graphics belong to the simulations of EF-Tu coming from *Thermus Aquaticus* unless otherwise stated (Figure 4.4-5). Compare to EF-Tu[H85(HIP)], EF-Tu[H85(HID)] has larger RMSD fluctuations. Especially in wild type H85(HID) simulation, there is a serious RMSD jump around 12ns. This is because of the Switch 1 region's conformational change. On the other hand, there is not such a dramatic conformational change in wild type H85(HIP) simulation. Further discussion on Switch 1 region motion will be in the Results and Discussion section. When we evaluate the RMSD graphs of all simulations, we realize that their RMSD values are similar to either Figure 4.4 or 4.5. Wild type H85(HIP) and (HID) simulations using the ff99SB; and also mutant H85A, D87E and T62A simulations' RMSD values have similar graph to Figure 4.4. On the other hand, wild type H85(HIE), mutant D21P, R57A, and D87EI61A simulations' RMSD values have similar graphs to Figure 4.5.

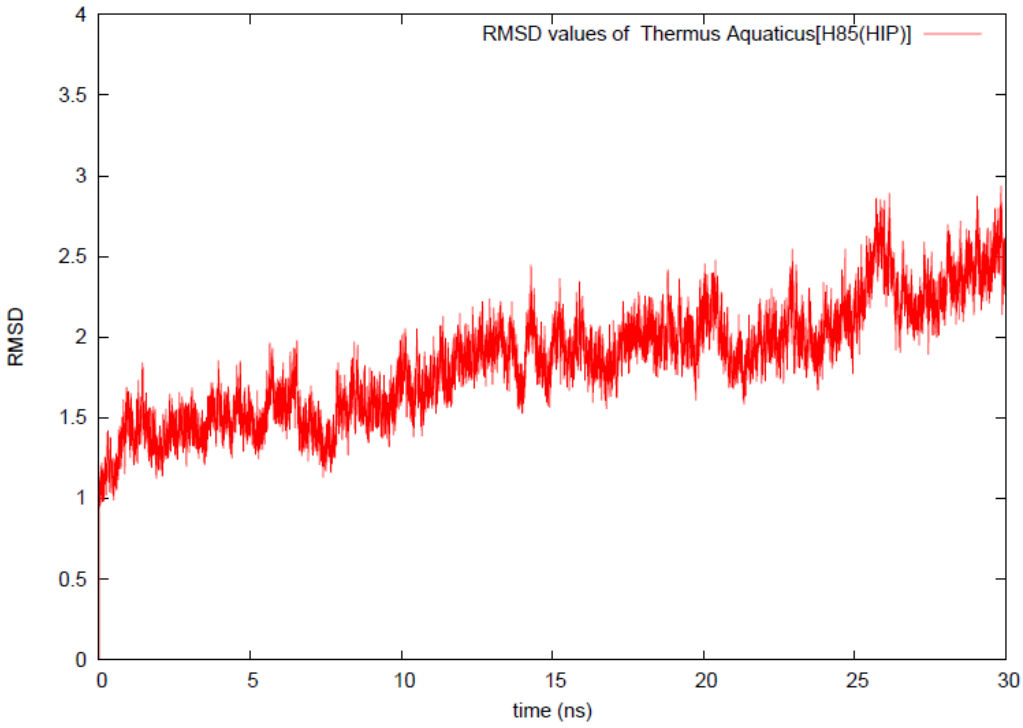

Figure 4.4. RMSD values of wild type EF-Tu[H85(HIP)] simulation.

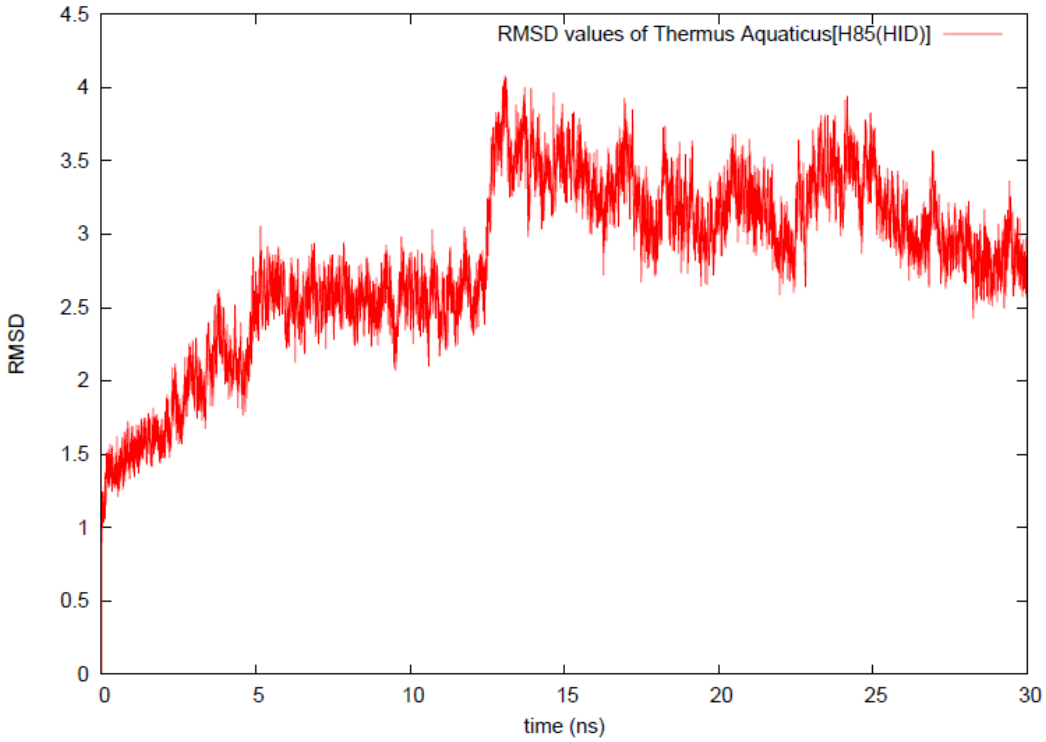

Figure 4.5. RMSD values of wild type EF-Tu[H85(HID)] simulation.

4.2. Effect of Histidine 85 Motion on GTP Hydrolysis

Histidine 85 is one of the most interesting residues around the catalytic site of EF-Tu. Available experimental data indicate a crucial role of H85 in the presence of ribosome, but not in the intrinsic hydrolysis reaction. While most researchers have suggested that H85 stabilizes the transiton state by properly orienting the attacking water molecule during hydrolysis, others have attributed it a general base role by abstracting a proton from the attacking water molecule.

We began our study by simulating different protonation states of H85 residue to investigate its behavior depending on the protonation states in EF-Tu·GTP complex (30ns simulations were performed for each protonation states). In the initial geometries of the system which are provided by the crystal structures coming from *Thermus aquaticus*, and *Escherichia coli*, H85 residue is located out of the catalytic site. However, as the

simulations proceeded, rotation of H85 toward the active site was observed, the amount of time spent in the active site being different among these three simulations (Figure 4.6-4.7).

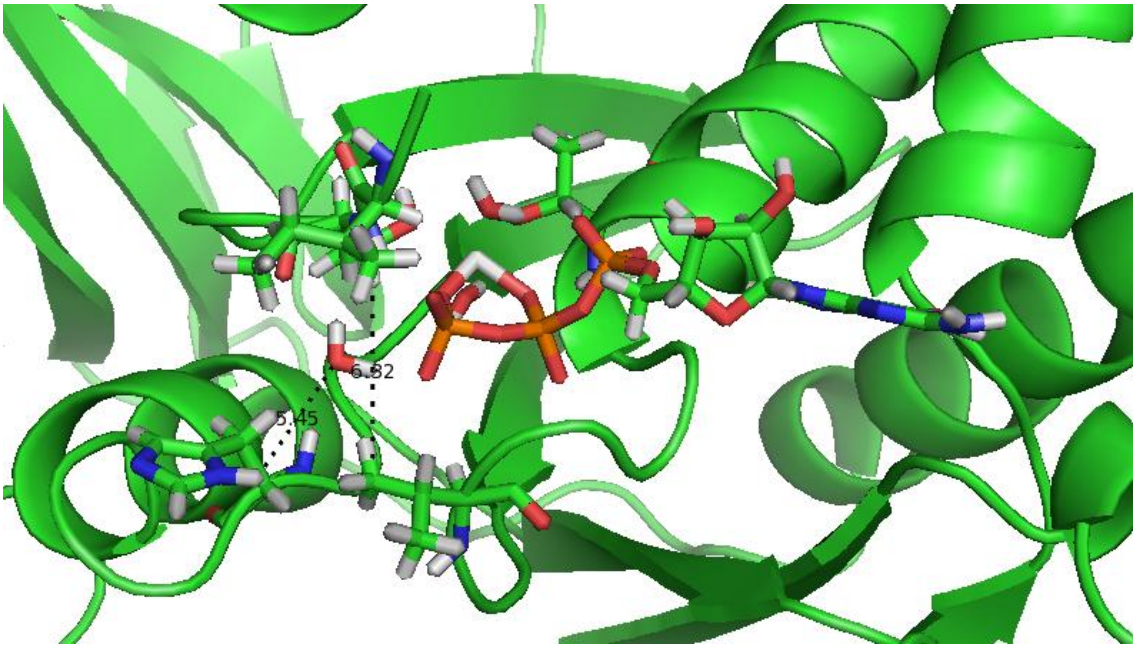

Figure 4.6. H85 (HID)out geometry.

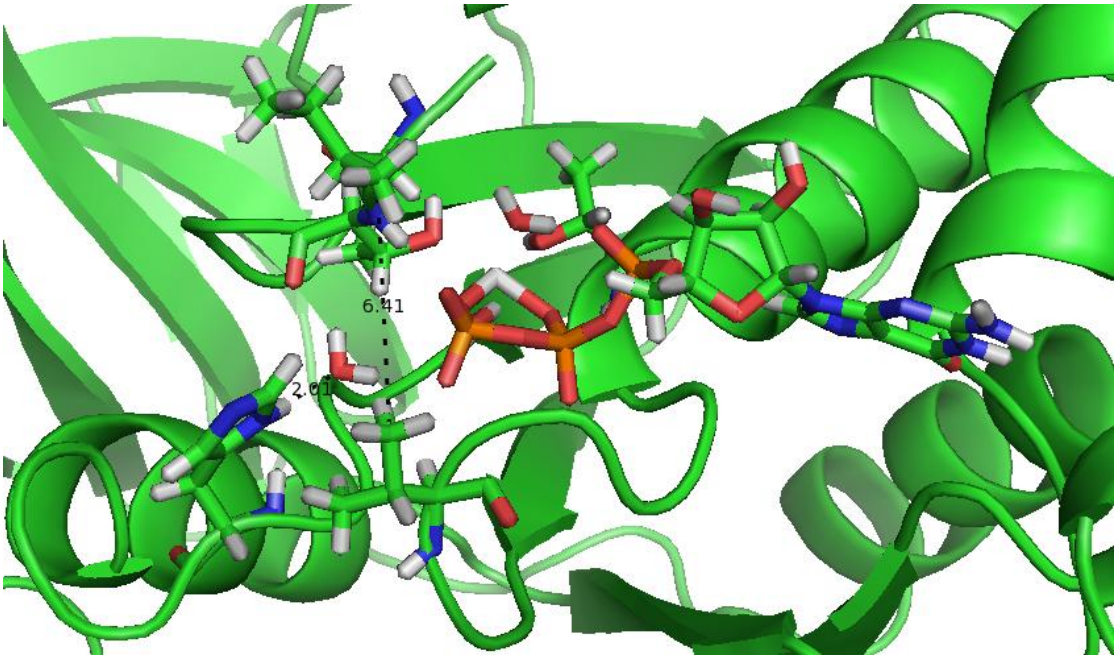

Figure 4.7. H85 (HID)in geometry.

The orientation of H85 to the active site just depends on the rotation around the histidine C_α-C_β bond. To determine the time spans at "in" and "out" positions, the dihedral C-C_α-C_β-C_γ of H85 was analyzed. Dihedral values that oscillate between 50 and 80 degrees represent the "out" conformation of H85 residue. The values above 120 degree represent the "in" conformation. Similar dihedral values were obtained for H85 (HID) and (H85) HIE forms; however, different results were observed for H85 (HIP) form (Figure 4.8-4.10).

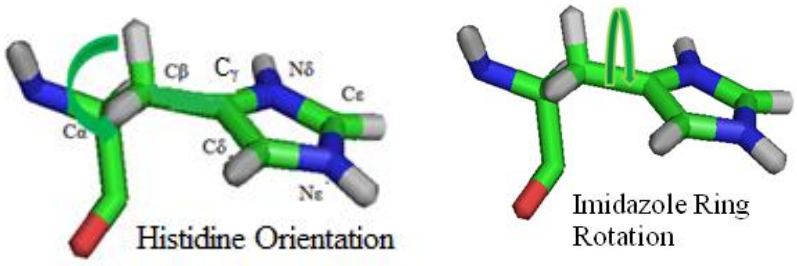

Figure 4.8. Motions of histidine residue.

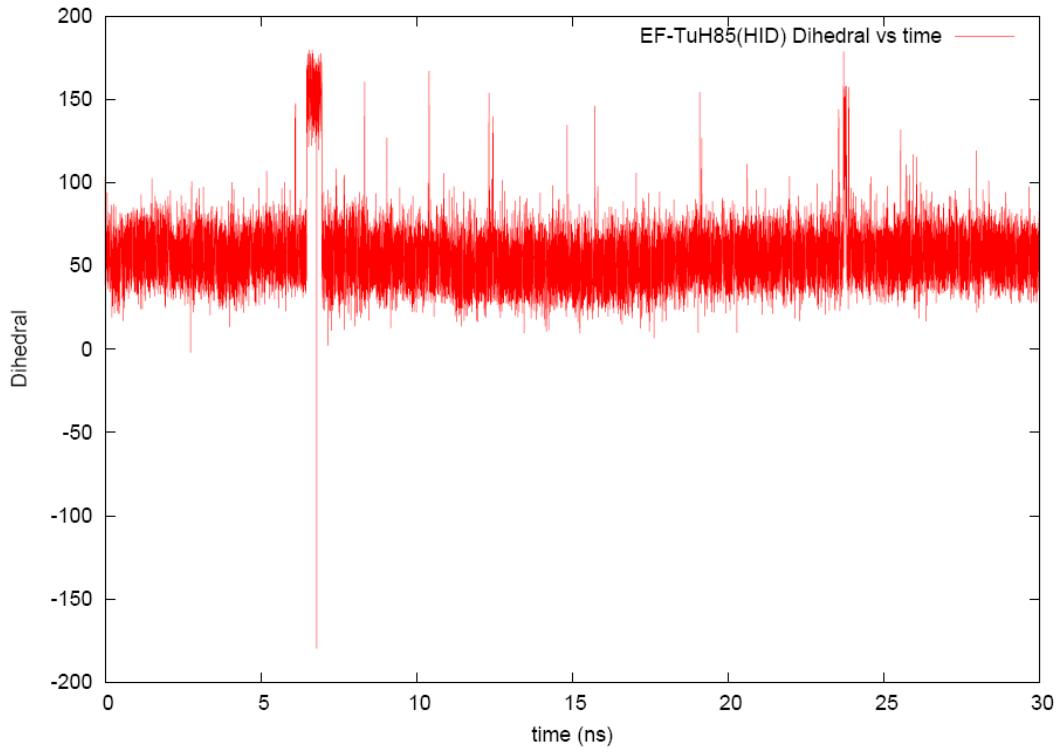

Figure 4.9. Dihedral C-C_α-C_β-C_γ of H85(HID) vs time.

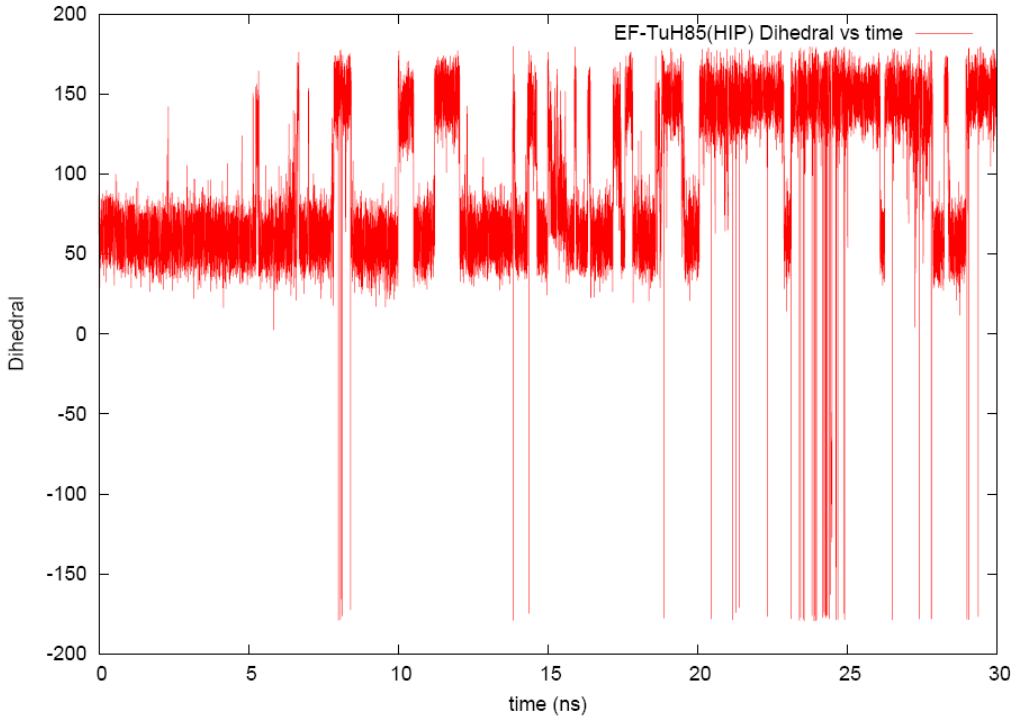

Figure 4.10. Dihedral C-C_α-C_β-C_γ of H85(HIP) vs time.

While H85 (HID) and H85 (HIE) forms (data not shown) turn into the active site for a limited time, H85 (HIP) tends to get close to the catalytic site more. It is probably because of the interaction between the (+) charge of H85 (HIP) and the (-) charges of GTP nucleotide phosphate group(s).

In previous studies, V20 and I61 residues were called as the "hydrophobic gate" which inhibits H85 rotation into the active site. Because different protonation states of the H85 residue have different orientation tendencies into the active site, we wanted to examine the hydrophobic gate phenomenon and try to get a correlation between the gate distance and the protonation state of H85. However, when we analyze the hydrophobic gate gap in these wild type simulations, there is no such a correlation between the gap and the H85 protonation state (Figure 4.11). The gate almost has enough space to host a hydrophilic histidine residue in all three simulations. A 9-10Å gap allows a histidine residue to be located between the wings of the gate. The time period in the active site depends on the attraction between H85 and the phosphate groups but does not depend on the gate distance. Stronger electrostatic interaction, between the positively charged residue

H85 (HIP) and the negatively charged phosphate groups, which is not present in the HID and HIE forms, lead to different time spans in the active site. In addition to this, some other factors, i.e. ribosome binding, may affect the gate distance, and the position of H85. However, protonation state of H85 alone also has an influence on its location.

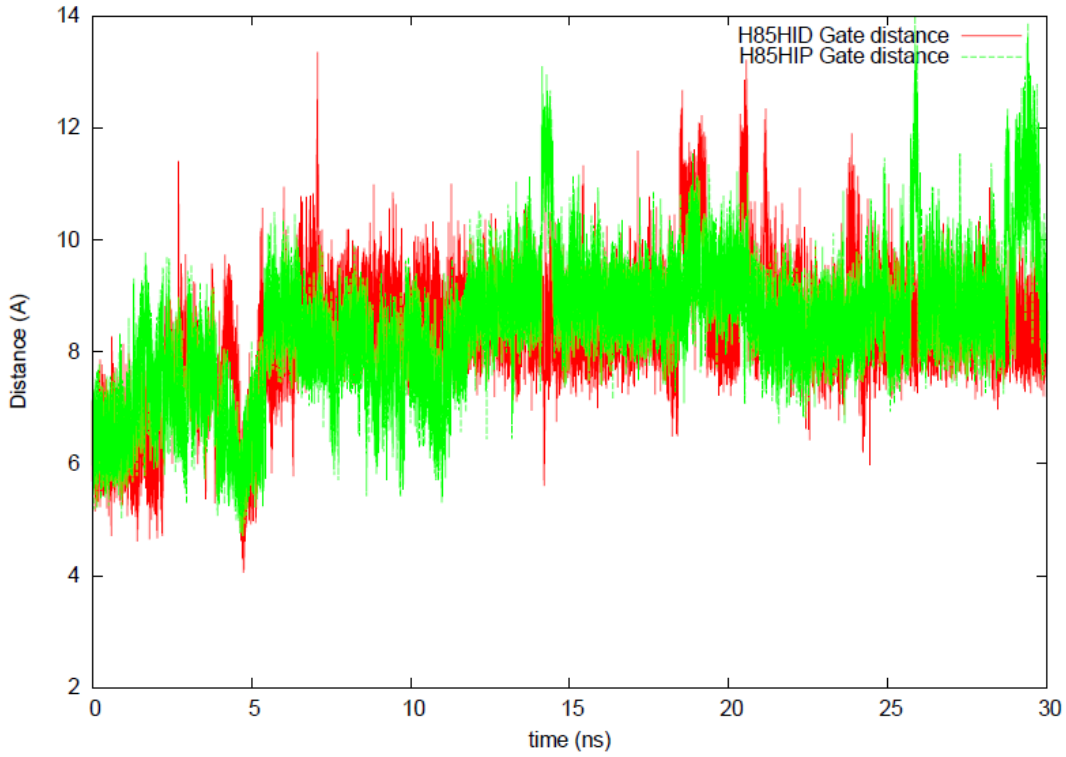

Figure 4.11. Distance between V20 and I61 residues (center of geometry of side chain C atoms were taken), in H85 (HID) and H85 (HIP) wild type simulations.

For further validation of this hypothesis, we performed EF-Tu[H85A] simulation, because alanine is a hydrophobic residue and would not tend to get into the active site. In this simulation we got the most closed V20-I61 distance (Figure 4.12). The gate distance showed great stability around 7Å. So we conclude that, the gate distance is directly related to hydrophilic property of the histidine residue and also its electrostatic interaction with GTP.

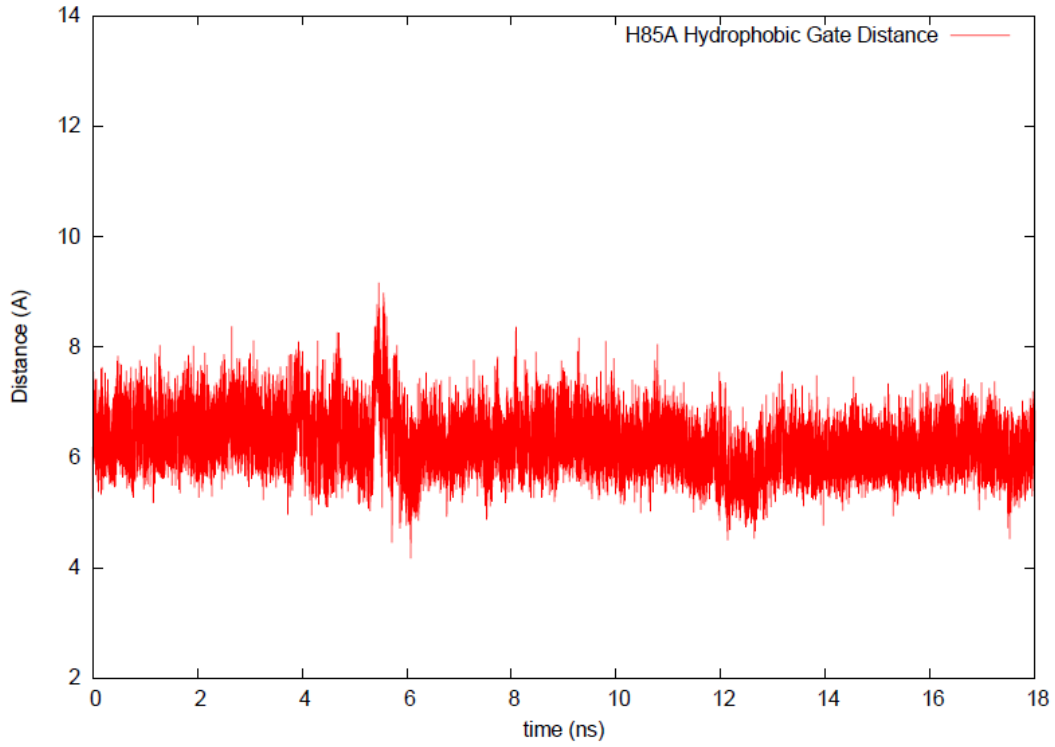

Figure 4.12. Distance between V20 and I61 residues (center of geometry of side chain C atoms were taken), in H85A mutant simulation.

In addition to the above observations, another interesting result comes out about the H85 imidazole ring behavior from these simulations. In addition to the orientation of H85 into the active site, rotation of imidazole ring is another intriguing point. Although H85 spent some time into the catalytic site to fulfill its role in the intrinsic GTP hydrolysis, its rotation about the C_β-C_γ bond (which is independent from the H85 protonation state), may be a drawback because, unless the ring gets a stable geometry it would be difficult to orient correctly the attacking water molecule. We traced C_α-C_β-C_γ-N_δ (Figure 4.8) dihedral of the imidazole ring in wild type simulations of H85 (HIP) and (HID) forms, and ended up with the following graph which represents the continuous rotation of the ring (Figure 4.13). N_δ of H85 is located in the active site for positive dihedral values of C_α-C_β-C_γ-N_δ. On the other hand, negative dihedral values for these analyses represent the rotated position of imidazole ring and C_δ or N_ε were positioned into the active site when H85 turns into the active site. The dihedral values showed a huge oscillation in 40^0-110^0 range, and there are also oscillations in the negative values in a large range.

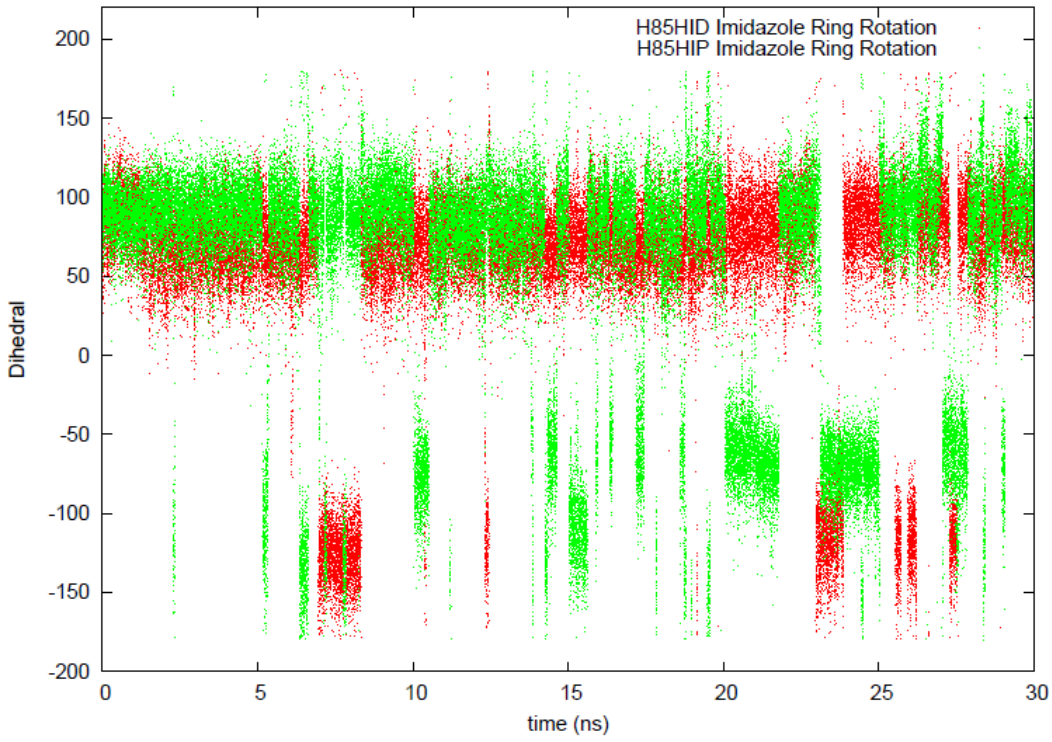

Figure 4.13. C_α-C_β-C_γ-N_δ dihedral analyses of H85 (HIP) and (HID) imidazole ring.

4.2.1. Effect of Aspartate87 Mutation to Glutamate (D87E) in Histidine85 Motion

Related to the role of H85, in an experimental study [53] aspartate 87 was mutated to glutamate (D87E), and an increase in intrinsic GTP hydrolysis was observed. We simulated EF-Tu[D87E] to analyze the effect of this mutation. Because glutamate has one more carbon atom in its side chain than aspartate, it is assumed that, E87 would move H85 into the active site by forming a salt bridge, increasing the GTP hydrolysis rate. We used two different H85 protonation states in our simulations, H85 (HID) and H85 (HIP). In H85 (HID) form, the interaction between E87-H85 was observed for a short time. Distance analysis between the side chain carboxyl carbon of E87 and N_δ of H85 was done (Figure 4.14). Average of 7Å distance represents the poor interaction between E87 and H85 residues. And similar to wild type EF-Tu[H85(HID)], H85 of EF-Tu[D87E] mutant is oriented into active site rarely (data not shown).

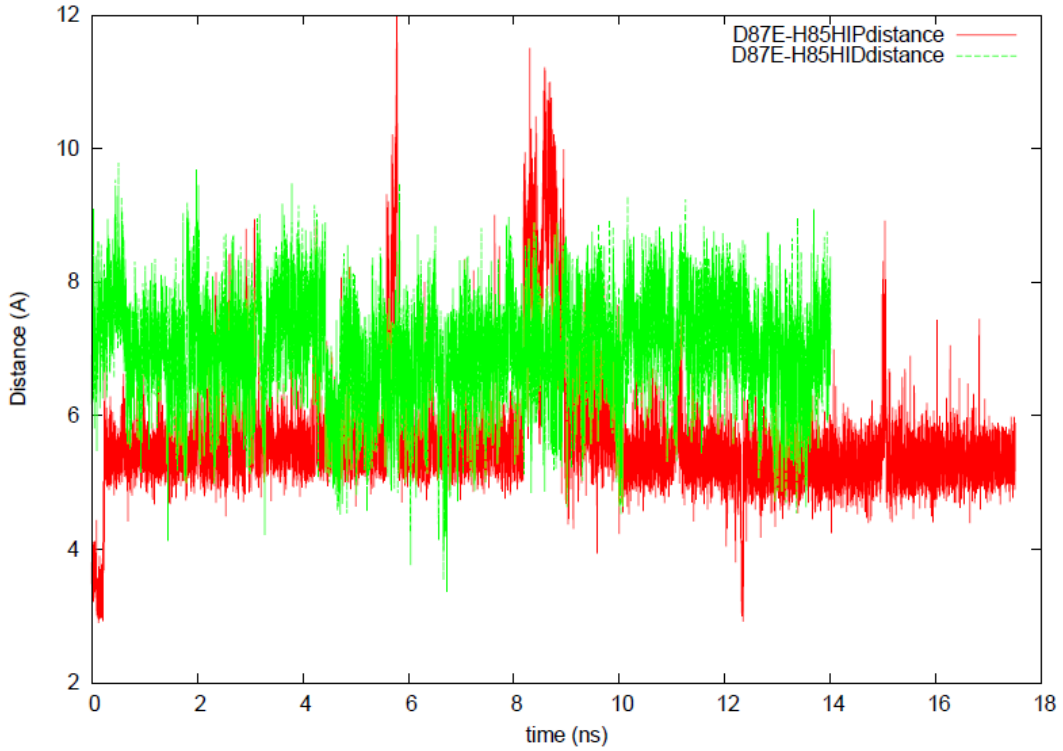

Figure 4.14. Distance between side chain carboxyl carbon of E87 and N_{δ} of H85 HID and HIP forms.

Having detected the short time interaction between H85 (HID) and E87, we have performed another simulation of EF-Tu[D87E] with H85(HIP) form. Similar to wild type EF-Tu[H85(HIP)], H85 (HIP) of EF-Tu[D87E] spent more time into the active site. Similar analyses were done and longer interaction time between E87 and H85 were observed (Figure 4.14). The Average 5Å distance shows the salt bridge between the E87 and H85 residues. However, during the simulation sometimes the interaction between these residues has been lost as a result of the E87 residue rotation toward the solvent. The distance values which are higher than 8Å represent that time period.

E87 may mimic the role of ribosome to some extent by holding H85 (HIP) into active site for longer time (Figure 4.15). On the other hand, there are two more observations related to this and wild type EF-Tu H85(HIP) simulations; i) H85 with HIP form can stay into the active site even in the absence of E87 interaction, ii) when E87 interacts with H85, the imidazole ring rotates less (Figure 4.16). Less rotation means better

orientating the water molecule(s) in the active site. So, increase in the rate may be attributed to the limited ring rotation. In wild type simulation of EF-Tu with H85 (HIP) form, the dihedral angle value responsible for ring rotation indicated more than 150^0 range, on the other hand, ring rotation in simulation of EF-Tu[D87E] mutant oscillated in a narrower range. In addition to the above observations, another important fact is the interaction between the hydrogen of C_δ atom and the water molecule in the active site when E87 and H85 form a salt bridge. If this interaction would occur between thehydrogenof N_ε and water molecule, it will be more meaningful. Probably, there is another conformation in which the interaction between the hydrogen of N_ε and water molecule occurs, just before the hydrolysis and we could not observe in our simulations.

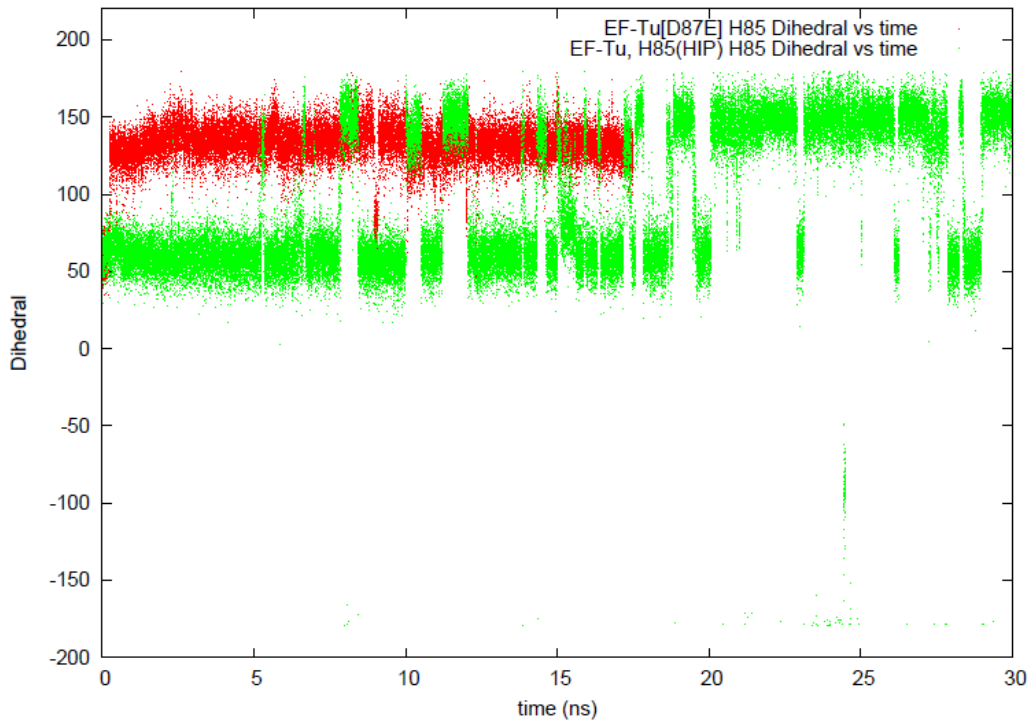

Figure 4.15. C-C_α-C_β-C_γ dihedral analyses of H85 of EF-Tu, H85(HIP) and EF-Tu[D87E].

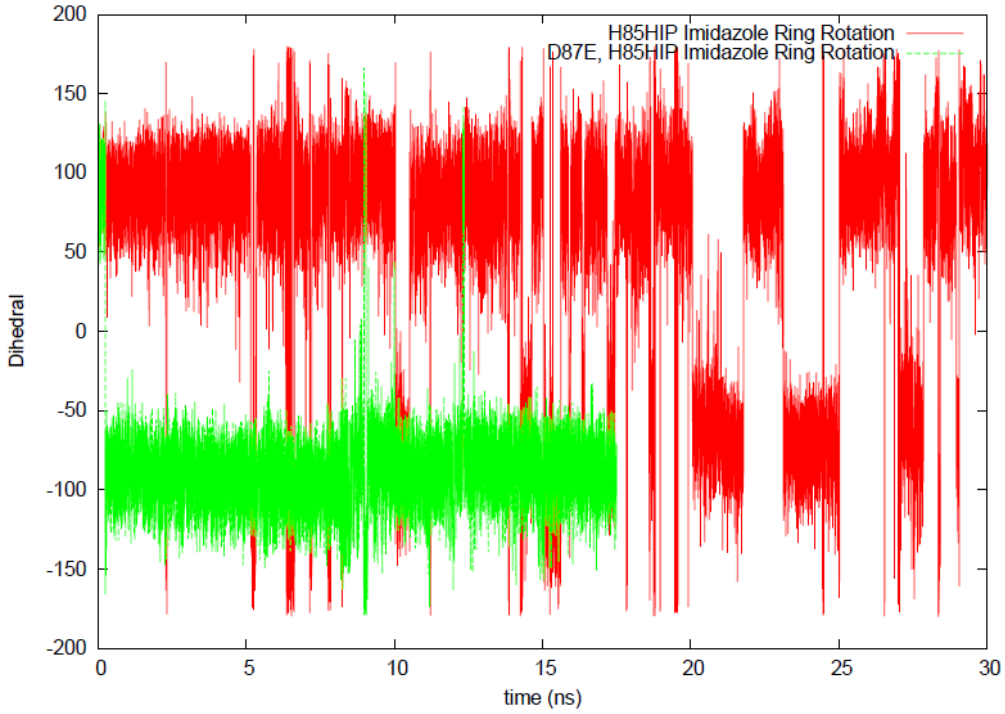

Figure 4.16. C_α-C_β-C_γ-N_δ dihedral analyses of wild type H85 (HIP) and D87E mutant H85 (HIP) imidazole ring.

4.2.2. Effect of I61 and V20 ("Hydrophobic Gate" Residues) in Histidine 85 Motion

Related to the H85 and imidazole ring motion, we have run another simulation of EF-Tu with aspartate 87 mutated to glutamate [D87E] and isoleucine 61 mutated to alanine [I61A]. We aimed at getting a more detailed and comprehensive information about the factors which cause the orientation of H85 into the active site and its imidazole ring rotation by simulating the doubly mutated EF-Tu. One of these mutations was to remove one wing of the hydrophobic gate, (I61A). In an experimental study isoleucine 61 was mutated to alanine, and in contrast to the expectations, the rate of GTP hydrolysis decreased [25]. We wanted to determine the exact role of I61 whether it is a barrier for H85 to be in contact with the active site, or it has another mission. And the second mutation was the D87E mutation. As discussed above, this mutation causes a salt bridge formation between H85 and the glutamate and prevents the H85 imidazole ring rotation to some extent. An experimental study indicates a decrease in hydrolysis rate, so only the

presence of H85 in the active site is not enough to increase the rate but there must be other factor(s) which affect the rate. These so called 'hydrophobic gate' residues, I61 and V20, may have other role(s).

We analyzed imidazole ring rotation in our double mutant simulation (Figure 4.17). In comparison to D87E mutation simulation, much more fluctuation of the H85 imidazole ring dihedral values has been observed which indicates more rotation. This may be interpreted as the follows; I61 is not real a barrier for H85 orientation into the active site, instead it hinders the imidazole ring rotation after the H85 residue turns into the active site.

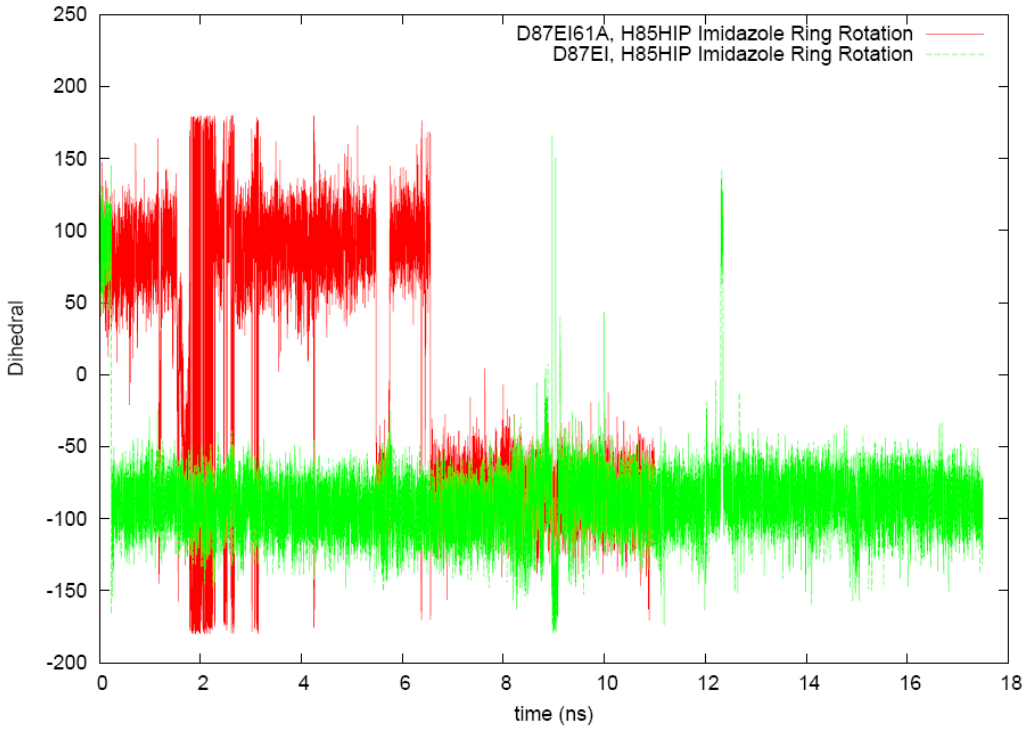

Figure 4.17. C_α-C_β-C_γ-N_δ dihedral (imidazole ring) analysis of D87EI61A and D87E mutant H85 (HIP) imidazole ring.

In another experimental study of a Ras-like GTPase, Rab5, ended up with an important result. Ala30 of Rab5 (or the equivalent position in other GTPases, e.g. Gly13 of Ras; Asp21 of EF-Tu) forms a H-bond with the β-γ atom. Because the main chain amide hydrogen of Ala30 is located near the beta-gamma bridge oxygen, it was thought as an H-bond donor and would compensate the charge accumulation on the bridge oxygen in the

transition state of GTP hydrolysis. Nineteen substitution mutations have been introduced at this residue and only the Pro substitution, which changes the backbone amide to an imide group that can no longer donate hydrogen bond, drastically reduces GTP hydrolysis rate by an order of magnitude [54]. We simulated the corresponding mutation in EF-Tu, [D21P].

At the starting point of the simulation V20-P21 peptide bond was in the trans form. However, as the simulation proceeded, steric effects of residues around the P21 residue forced a trans-cis isomerization of the peptide bond between P21 and V20. In general, all peptide bonds assume a trans form. However, glycine, which has only hydrogen as a side chain, and proline, which has a cyclic structure with its side chain, may form cis peptide bonds (Figure 4.18).

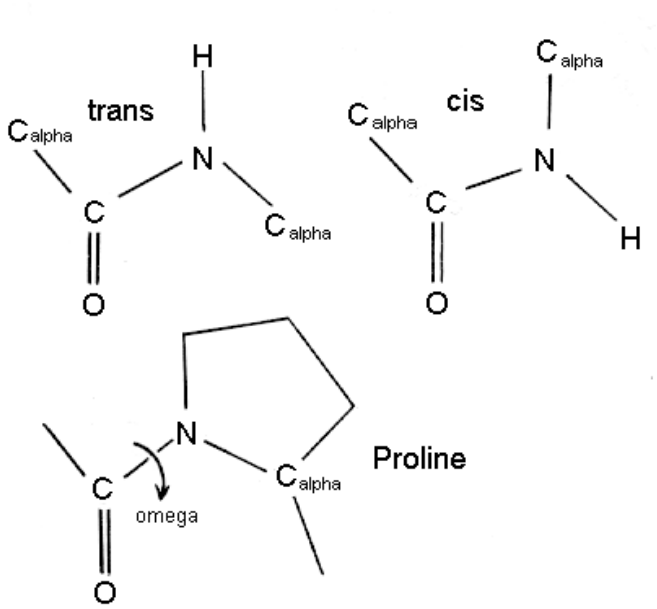

Figure 4.18. Trans-cis peptide bonds and proline strucuture.

V20 is a wing of the hydrophobic gate and the cis peptide bond formation caused a displacement of V20 from the initial position and the distance between side chains of H85 and V20 increased almost by 1Å (Figure 4.19-22). This motion leaded less steric crowdedness around the H85 and let imidazole ring to rotate more freely (Figure 4.21). As a result, the D21P mutation caused the absence of an H-donor, and also provided an environment for continuous rotation of H85 imidazole ring. As the experimental study

suggests, the loss of the H-donor might affect the rate, but also the continuous rotation of the imidazole ring might decrease it, too.

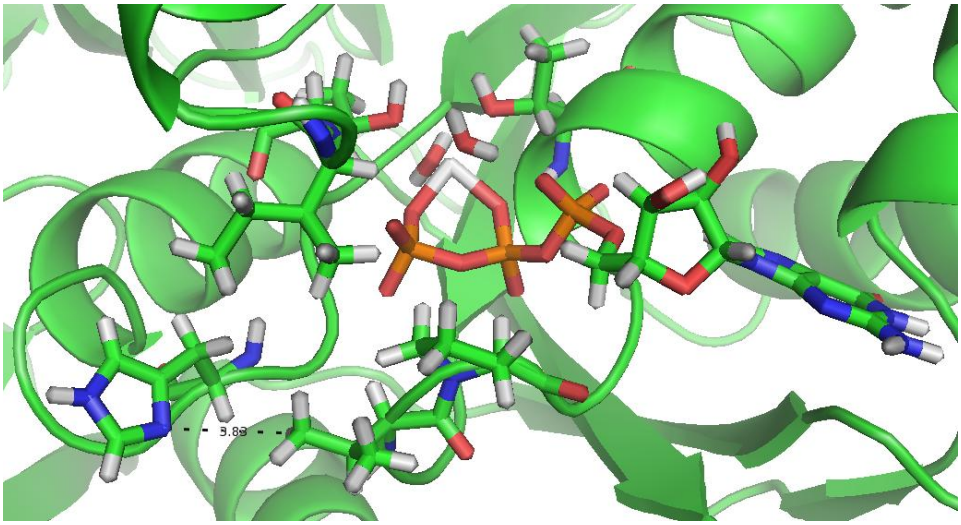

Figure 4.19. Initial geometry of EF-Tu[D21P], distance between H85-V20 is shown.

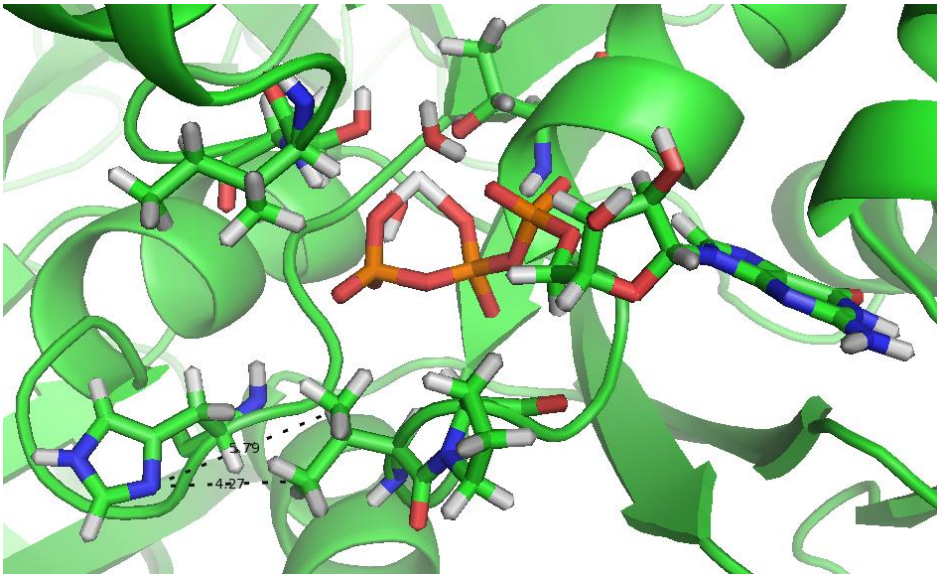

Figure 4.20. Geometry of EF-Tu[D21P] after 1ns, distances between H85-V20 are shown.

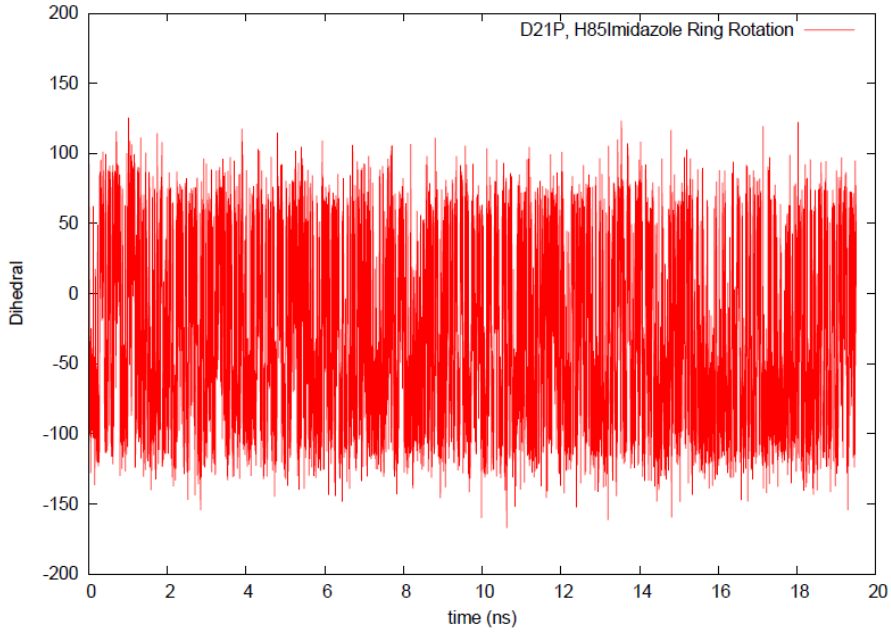

Figure 4.21. C_α-C_β-C_γ-N_δ dihedral analyses of D21P mutant H85 imidazole ring.

Taking all information into account about the "hydrophobic gate" story, we claim that, the mission of V20 and I61 amino acid residues is not forming a barrier for H85 to rotate, but assisting the hydrolysis by holding the H85 imidazole ring, preventing its rotation, like a clamp. Two steps are necessary for activity of H85 in GTPase activity of EF-Tu, i) orientation towards the active site, ii) stable positioning in the active site.

As shown above, the protonation state of H85 affects the time it spends in the active site. Interaction with a negatively charged residue (D87 in the wild type, glutamate in the D87E mutant) may lead to the protonation of H85. In the mutant, such an interaction is almost always present during the simulation. Hence, although we have not computed the pK_a of H85, one may expect an elevated pK_a for this residue. In the wild type, the shorter size of the aspartate does not allow such an interaction. However, the presence of ribosome may position the aspartate close to the histidine, increasing its pK_a. Moreover, the negative charges on the ribosomal RNA may favor the protonation of H85. As stated before, H85 residue has very critical role in GTP hydrolysis in the presence of programmed ribosome. In addition, the arginine 59 residue which is located in the Switch 1 region, has been found experimentally to have an important role in EF-Tu binding to the ribosome. In the presence of the ribosome R59 would probably bind EF-Tu to the ribosome, similar to an anchor and

after this binding H85 will be oriented into the active site by the ribosome and "hydrophobic gate" residues will get close and hold H85 tightly and aid the hydrolysis.

4.3. Switch 1 Motion

Another interesting finding of our simulations is about the behavior of Switch 1 region, and also D51 and T62 residues which are thought to be responsible for holding the position of Switch 1 region in EF-Tu. In the crystal structures of EF-Tu, both from *Thermus aquaticus* and *Escherichia coli*, T62 coordinates with Mg^{++} ion directly. D51 is also in coordination with the Mg^{++} ion via a water molecule and directly connected to the T62 side chain hydroxyl group with an H-bond (Figure 1.10). In all of the simulations both on the wild type and mutant EF-Tu, D51 moved away from its original position in the crystal (Figure 4.22-4.24). Although D51 showed significant displacement throughout the trajectory, there is no direct correlation between the motion of D51 and Switch 1 region.

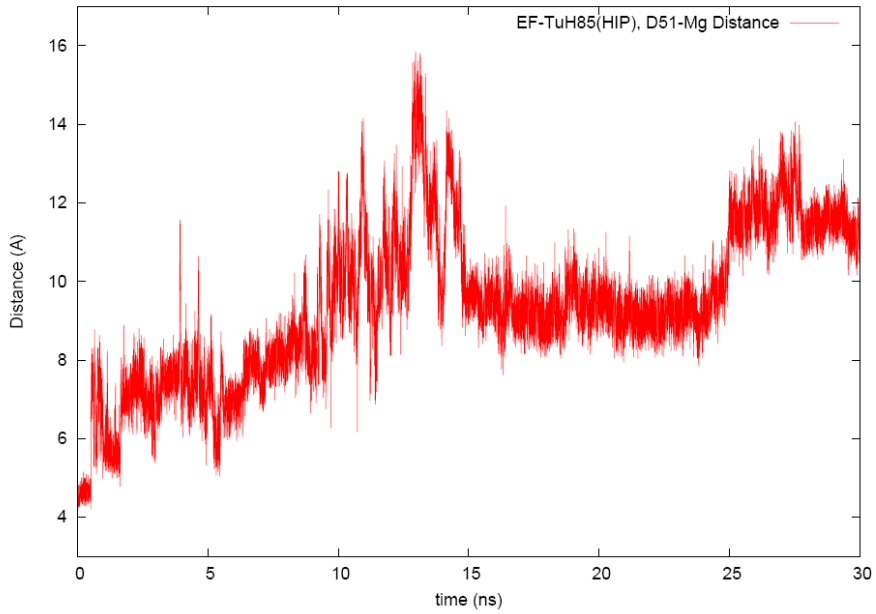

Figure 4.22. Distance between carboxyl carbon atom of D51 and Mg++ ion throughout the EF-TuH85(HIP) simulation.

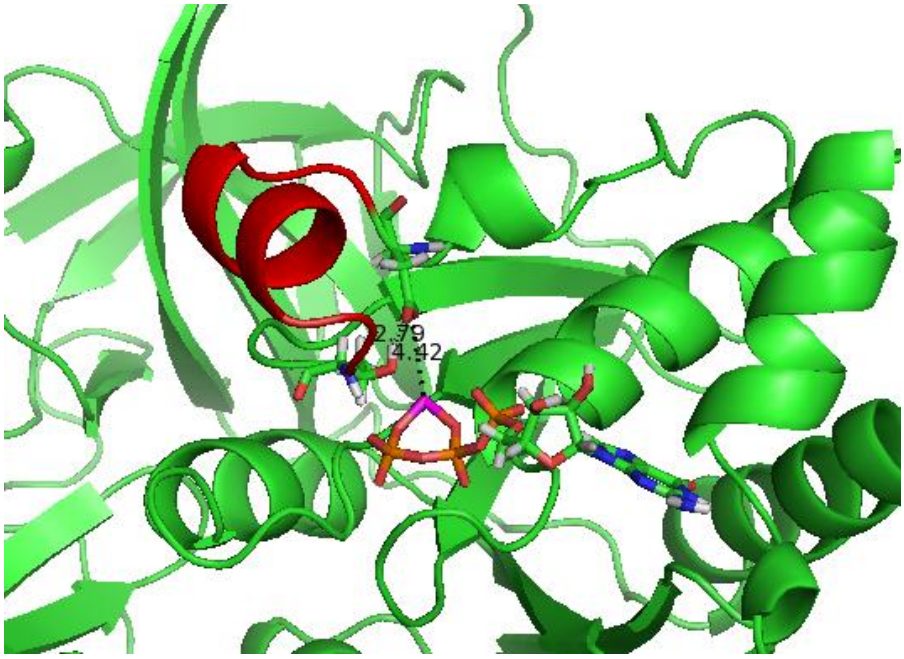

Figure 4.23. Initial position of D51 and T62 residues in wild type EF-TuH85(HIP) simulation, Switch 1 region is shown in red.

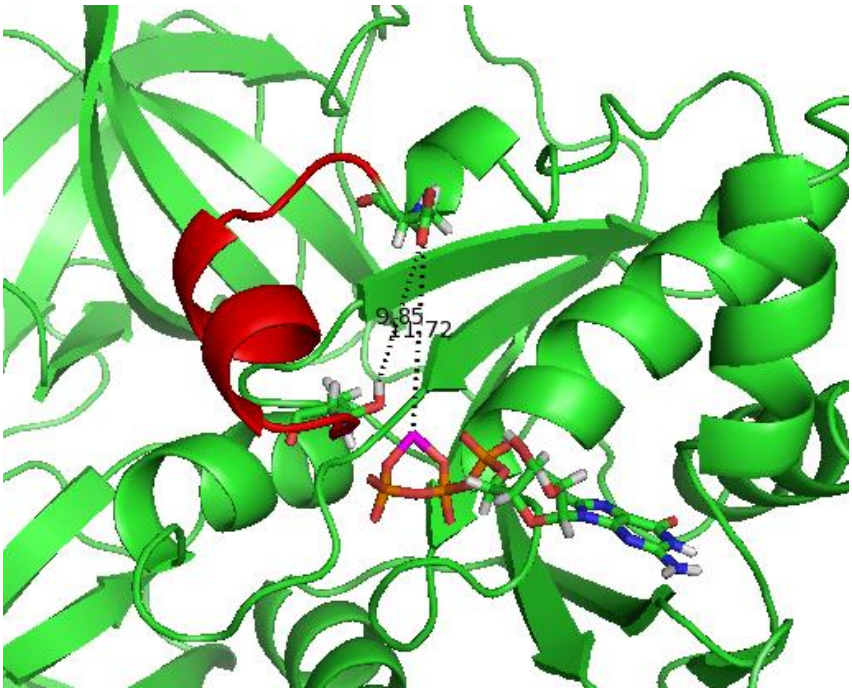

Figure 4.24. Position of D51 and T62 residues in wild type EF-TuH85(HIP) simulation after 10 ns, Switch 1 region is shown in red.

We tried to explain the reason of the D51 displacement from its original position seen in the crystal. After visually inspecting the MD trajectories, our initial assumption was that the interaction between the negatively charged D51 and positively charged arginine 57 was increasing the mobility of D51. Early in the simulations they were in contact with each other, form a salt bridge and the displacement of D51 occurs. They also keep their interaction, through most of the trajectory. To test this hypothesis we mutated R57 to alanine (R57A) and simulated. In the absence of the positively charged R57 residue, one of the twelve Na^+ ions which were added to neutralize the medium at the beginning, interacted with D51 which left its initial position. This suggested that any nearby positive charge induced the D51 motion. To further examine this, in addition to R57A mutation, Rubidium (Rb^+) ions were used to neutralize the media instead of Na^+. Rubidium (Rb^+) ions have much larger size than Na^+ ions, and they would not fit to small holes unlike Na^+. As a result, we expected that the Rb^+ ions could not interact with D51 and displacement would not occur. Our results from EF-Tu[R57A(Rb)] simulation showed partly parallelism to our expectation. Rb^+ ions could not interact with D51, however, even in the absence of any positive charge D51 moved from its original position.

Then we investigated the role of the threonine 62 residue which was thought to behave, similar to D51, having a critical role for positioning the Switch 1 region. We simulated its alanine mutant, EF-Tu[T62A]. This mutant showed a dramatic motion of Switch 1 region even in the early time period of the simulation, in such a way that, Switch 1 goes to the EF-Tu·GDP like conformation observed in the crystals. For complete transition to the GDP conformation, the motions of Switch 2, Domain 2 and 3 are necessary, but this mutation showed how important the presence of T62 and its interaction with the Mg^{++} ion for the EF-Tu·GTP conformation and Switch 1 position is (Figure 4.25-28 and 4.6). So according to our results, D51 is not a critical residue for positioning the Switch 1 region, but T62 is responsible from holding its place.

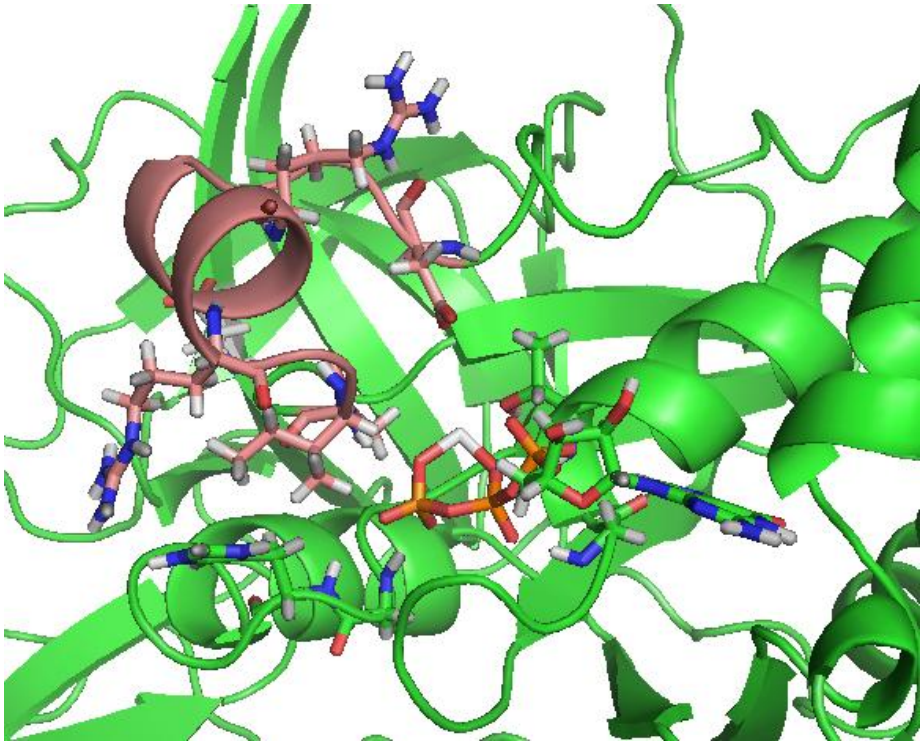

Figure 4.25. Initial geometry of EF-Tu[T62A] structure, Switch 1 is shown in pink.

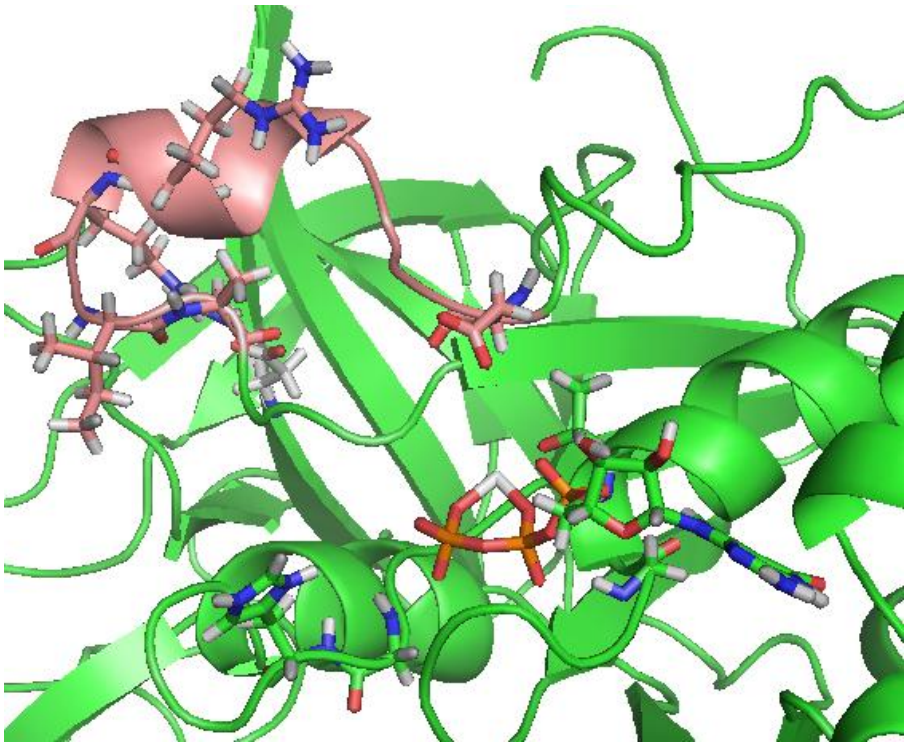

Figure 4.26. Geometry of EF-Tu[T62A] structure after 5ns, Switch 1 is shown in pink.

Another striking result is the motion of Switch 1 region. In most of our simulations, Switch 1 region showed serious displacement and conformational changes, e.g. in wild type simulations of *E.coli* and *Thermus Aquaticus* EF-Tu[H85(HID)]; and D21P, R57A mutant simulations (Figure 4.27). On the other hand we cannot rule out the Switch 1 conformational change possibility for other simulations, based on the observations of maximum 30ns time periods. In contrast the mobility of Switch 1 region in the simulations performed by using ff03 force field, there is not such a motion in the simulations performed by using ff99SB force field. The most fundamental difference between these force fields is that, ff03 stabilizes the α-helix structure more than the ff99SB. If the conformation of an α-helix can change in a simulation with ff03, it can also change in another simulation performed by ff99SB easily. That is to say, conformational changes observed in the simulations are not the artifact of ff03 force fields. It is possible to observe this motion if we carry on the simulations for larger time spans, especially for the ones performed by using ff99SB.

Conformational change of Switch 1 can be observed in different time periods of the simulations because of the flexibility of the region. On the other hand, early conformational changes imply that crystal contacts probably stabilize the α-helix structure of Switch 1 seen in the EF-Tu·GTP crystal. In solution, Switch 1 region is very mobile and during this motion R59 residue which is known to have a role as to bind EF-Tu and ribosome is quite far from its initial position seen in the crystal. The conformation of Switch 1 we have observed in our simulations, probably, is not the one which binds to the ribosome. However, the presence of t-RNA and ribosome may decrease the mobility and change the conformation by binding to R59 and other corresponding amino acids. This binding may stabilize the α-helix structure of Switch 1 and it is possible that, α-helix structure exists as minor conformation in solution, yet the presence of ribosome may lead this conformation as the major one.

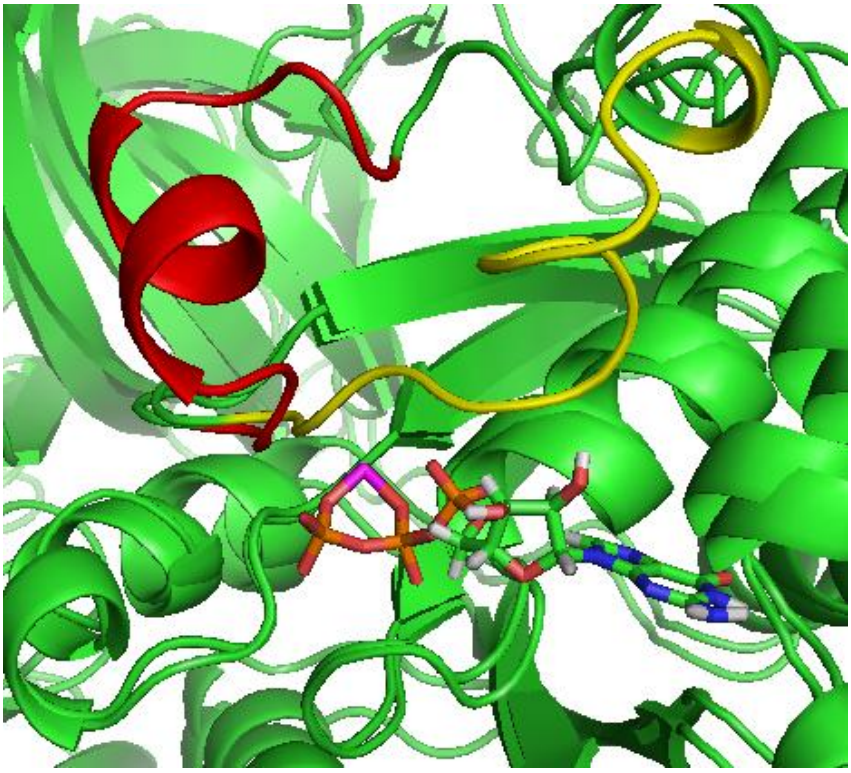

Figure 4.27. Motion of Switch 1 region in 14ns, from wild type EF-Tu[H85(HID)] simulation. Red cartoon represents the initial, yellow represents the final position.

We can also approach from different point of view to the Switch 1 region. In one of our simulations R57 gets close to the active site and contacts GTP. This arginine residue may be the lost "Arg-finger" in EF-Tu. It is possible that in the ribosome induced GTP hydrolysis another conformation of EF-Tu may exist and R59 binds to ribosome and flexible Switch 1 region may enable R57 contact with GTP. The conformation seen in the crystal structure of EF-Tu·GTP may not have a catalytic importance.

Two important findings from Switch 1 motion and T62A mutant simulation can be evaluated together. In an experimental study, EF-Tu structure has been determined just after the GTP hydrolysis, by an aid of antibiotic aurodox [30]. In this structure all Domains and Switches have the same orientation as in the GTP form, however residues between 52 and 65 which is the Switch 1 region, cannot be determined because of high disorder of the region. This is probably because of the displacement of T62 residue by any factor. Switch 1 region is already very dynamic and absence of T62 which is the unique residue holding

the Switch 1, probably let to more displacement of this region. When T62 losses its position Switch 1 area cannot be determined in the crystal.

Another interesting finding is about the motion of Switch 1 towards t-RNA binding site in our T62A mutant simulation. It is known that EF-Tu·GTP complex has higher binding affinity to t-RNA than EF-Tu·GDP form. In an experimental study crystal of Cys-tRNACys·EFTu·GDPNP ternary structure was determined [21], and when we align the crystal structure and a snapshot from T62A mutant simulation, Switch 1 motion to the t-RNA binding site can be clearly seen (Figure 4.28). As we metioned before, T62A mutant has a tendency to go to EF-Tu·GDP like conformation. When Switch 1 region occupies the t-RNA binding site, t-RNA cannot bind properly to the EF-Tu and EF-Tu·GDP conformation binding affinity to the t-RNA will decrease. This result also indicates the importance of T62 residue and its coordination to Mg^{++} in terms of t-RNA binding.

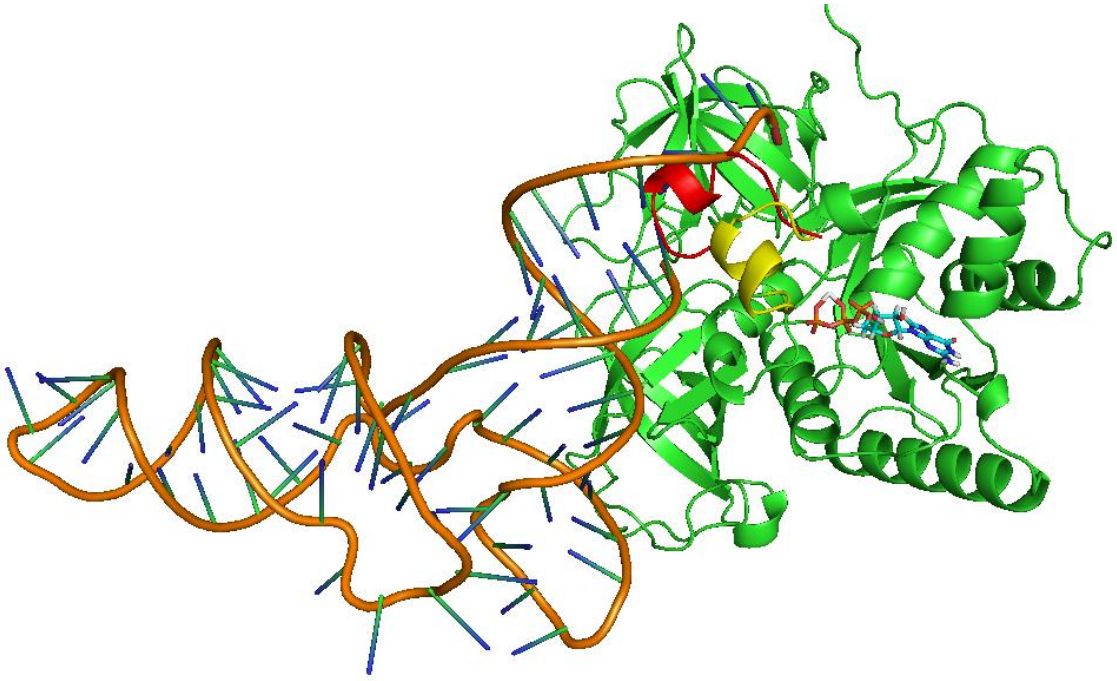

Figure 4.28. Cartoon representations of Cys-tRNACys·EFTu·GDPNP and a snapshot from T62A simulation. Yellow cartoon shows the Switch 1 in crystal, red cartoon shows the Switch 1 in T62A after 5ns simulation.

To validate the above observations, the wild type EF-Tu simulations with H85 (HIP) and H85(HID) were repeated by using a different force field, ff99SB. In addition, we have carried out a simulation with a larger solvent box, the shortest distance between the protein and the edge of the box being 20 Å. Similar results were obtained. Moreover, another crystal structure of EF-Tu coming from *E.coli* was used to simulate. This simulation has an importance from two different points of views; i) this new crystal comes from different organism, ii) these organisms need different optimum temperature for their biological activity. So we performed our simulation by using the crystal coming from *E.coli* at 310^0K. This means different kinetic energy of the system, so some observations might not be observed in this simulation. We run H84 (HIP) form and ended up parallel results and observations, such as displacement of D51 residue, with EF-Tu coming from *Thermus aquaticus* with H85 (HIP).

5. CONCLUSIONS AND SUGGESTIONS

In this study, wild type and mutant structures of the GTP form of Elongation Factor Tu (EF-Tu·GTP) were investigated by means of molecular dynamics simulations, in order to understand and explain the roles of important amino acid residues in the GTPase activity of EF-Tu. We mainly focused on the motion of Switch 1 region and the D51 residue and also possible functions of the T62, H85, V20 and I61 residues.

Our results indicated that the Switch 1 α-helix structure seen in the crystal structure is very unstable and dynamic when introduced into the solvent medium. Conformational changes of this region were observed in different periods of the simulations, showing the flexibility of the Switch 1 area.

Related to Switch 1 region, the roles of D51 and T62 residues were identified. In all of our simulations the D51 residue was very mobile and showed significant displacements throughout the trajectories. On the other hand, we could not detect any direct correlation between the motion of D51 and the Switch 1 region. However, T62-Mg^{++} interaction was determined as the main factor for holding the position of the Switch 1 region. In the absence of this interaction, the conformation of the EF-Tu showed a tendency to undergo a transition to an EF-Tu·GDP like conformation. It is known that the EF-Tu·GTP complex has a higher affinity to t-RNA, than the EF-Tu·GDP complex. The motion of Switch 1 towards the t-RNA binding site upon the loss of the T62-Mg^{++} interaction is probably responsible for the low affinity of the T62A mutant to t-RNA.

Other important findings of our study are about the H85 residue which is thought to have a role in the GTP hydrolysis reaction. In the crystal structures coming from *Thermus aquaticus* (1EFT) and *E.coli* (1OB2), H85 is seen to be outside the active site. In our simulations we observed the orientation of the H85 into the active site and the time spent in the active site depended on the protonation state of H85. Positively charged form of H85 was attracted by the negative charges of GTP and stayed in the active site more than the other two forms. Moreover, the V20 and I61 residues which are called as the

“Hydrophobic Gate” residues were thought as a barrier for H85 rotation towards the active site. We analyzed the relevance between the gate distance and the protonation state of the H85 residue and concluded that there is no relation between them. And the gate almost always has enough space to host the hydrophilic H85 residue in the active site. In addition to the orientation of H85, we also realized the importance of H85 imidazole ring rotation.

In one of the experimental studies, an increase in the GTPase activity of EF-Tu[D87E] mutant was reported. In our EF-Tu[D87E] simulation we found out that, the imidazole ring rotation decreased as a result of the salt bridge formation between the E87 and H85. In the literature, it was proposed that H85 stabilizes the transition state by orienting the attacking water molecule correctly. As a result of the decrease in the imidazole ring rotation, H85 may orient the water molecule more efficiently. This fact may explain, at least in part, the rate increase in the D87E mutant.

Although some early studies suggested that V20 and I61 prevent H85 orientation into the active site, V20G and I61A mutations caused a decrease in the GTP hydrolysis rate. To be able to explain this variance, we have simulated EF-Tu[D87E][I61A]. The analyses showed that absence of the I61 bulky side chain caused an imidazole ring rotation more than in EF-Tu[D87E]. Similar results were obtained from the EF-Tu[D21P] mutation. Nearly all amino acids form trans peptide bonds. However, because of the steric effects the P21 residue forms a cis peptide bond with V20. This trans-cis isomerization caused a displacement of V20 from its original position seen in the crystal and the distance between H85 and V20 was elongated by 1Å. This elongation removed the steric crowdedness around H85 and we observed much more imidazole ring rotation. This increase in the rotation may be one of the reasons of the decrease in the GTP hydrolysis rate. As a conclusion, V20 and I61 residues do not form a real barrier for the orientation of H85 into the active site. However they stabilize the H85 residue by squeezing it when it turns into the active site, probably this stabilization also happens in the presence of the ribosome.

The following suggestions can be made for future work:

- Extention of the present MD simulations.

- Calculating the pKa of His85 residue in wild type, in the presence of E87 and ribosome, individually.

- Elucidating the phosphate hydrolysis mechanism by applying QM/MM calculations.

APPENDIX A

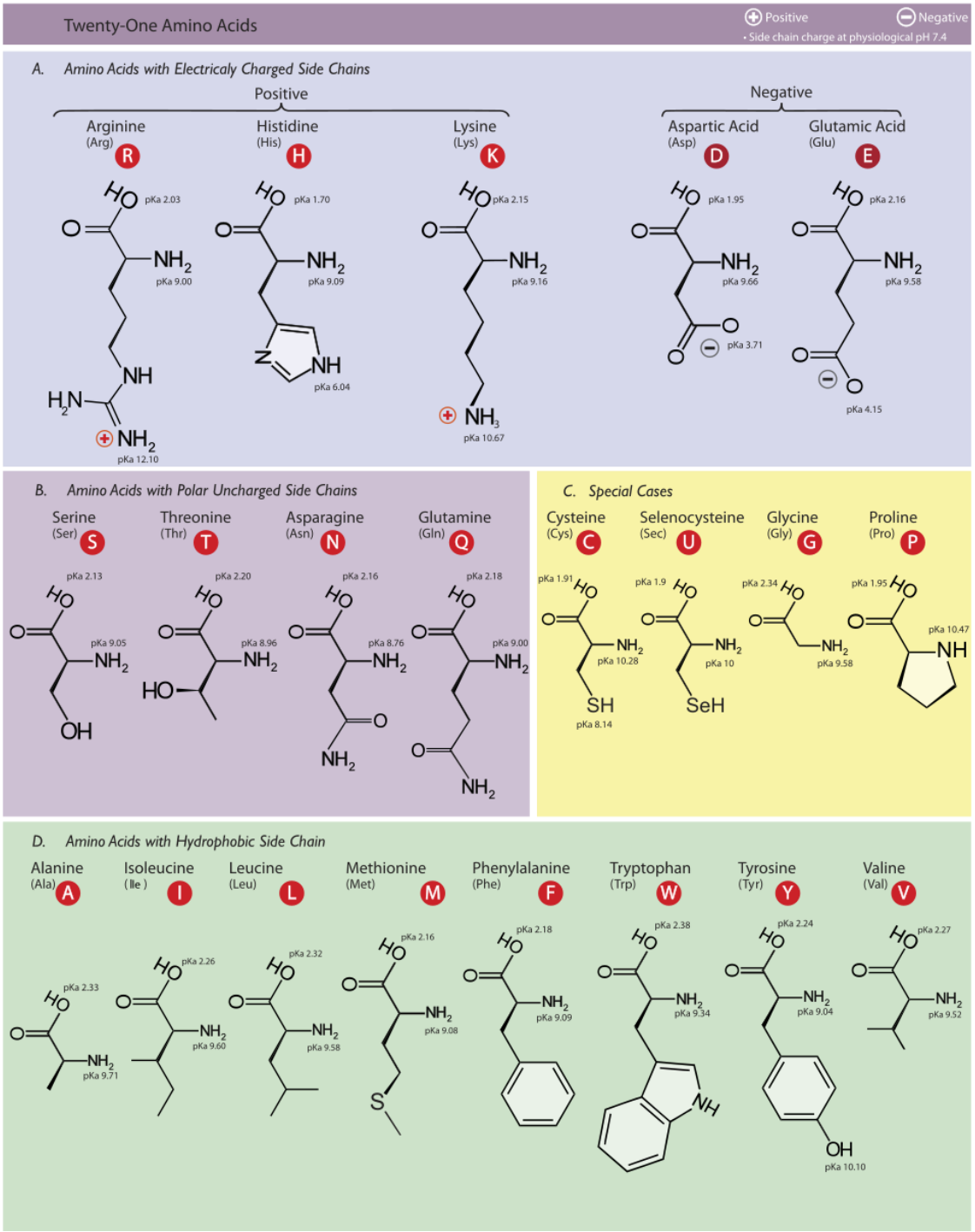

Figure A1. List of aminoacids [55].

REFERENCES

1. Spirin, A. S., "Ribosome as a Molecular Machine", *FEBS Lett.*, Vol. 514 (1), pp. 2–10, 2002.

2. Hauryliuk, V. V., "GTPases of the Prokaryotic Translation Apparatus", *Molecular Biology*, Vol.40 (5), pp. 688-701, 2006.

3. Kubarenko, A. V., Sergiev, P. V., Rodnina, M. V., "GTPases of the Translation Apparatus", *Mol. Biol.*, Vol. 39, pp. 746–761, 2005.

4. Maitra, U. S. E., Chaudhuri, A., "Initiation Factors in Protein Biosynthesis", *Annu. Rev. Biochem.*, Vol. 51, pp. 861–900, 1982.

5. Agrawal, R. K., Penczek, P., Grassucci, R. A., Frank, J., "Visualization of Elongation Factor G on the Escherichia coli 70S Ribosome: The mechanism of Translocation", *Proc. Natl. Acad. Sci. USA*, Vol. 95, pp. 6134–6138, 1998.

6. Noller, H. F., Yusupov, M. M., Yusupova, G. Z., Baucom, A., Cate, J. H., "Translocation of tRNA During Protein Synthesis", *FEBS Lett.*, Vol. 514, pp. 6–11, 2002.

7. Rodnina, M. V., Pape, T., Fricke, R., Wintermeyer, W., "Elongation factor Tu, a GTPase Triggered by Codon Recognition on the Ribosome: Mechanism and GTP Consumption", *Biochem. Cell. Biol.*, Vol. 73, pp. 1221–1227, 1995.

8. Stark, H., Rodnina, M. V., Rinke-Appel, J., Brimacombe, R., Wintermeyer, W., van Heel M., "Visualization of Elongation Factor Tu on the Escherichia coli Ribosome", *Nature*, Vol. 389, pp. 403–406, 1997.

9. Freistroffer, D. V., Pavlov M. Y., MacDougall, J., Buckingham, R. H., Ehrenberg, M., "Release Factor RF3 in E. coli Accelerates the Dissociation of Release Factors RF1 and RF2 from the Ribosome in a GTP-dependent Manner", *EMBO J.*, Vol. 16, pp. 4126–4133, 1997.

10. Zavialov, A. V., Buckingham, R. H., Ehrenberg M., "A Posttermination Ribosomal Complex is the Guanine Nucleotide Exchange Factor for Peptide Release Factor RF3", *Cell.*, Vol. 107, pp. 115–124, 2001.

11. Krab, I. M. and A. Parmeggiani, "EF-Tu, A GTPase Odyssey", *Biochimica et Biophysica Acta*, Vol. 1443, pp. 1-22, 1998.

12. Krab, I. M. and A. Parmeggiani, "Mechanisms of EF-Tu, A Pioneer GTPase", *Progress in Nucleic Acid Research and Molecular Biology*, Vol. 71, pp. 513-551, 2002.

13. Boguski, M. S. and F. McCormick, "Proteins Regulating Ras and Its Relatives", *Nature*, Vol. 366, pp. 643-654, 1993.

14. Sprang, S. R., "G Protein Mechanism: Insights from Structural Analysis", *Annu. Rev. Biochem.*, Vol. 66, pp. 639-678, 1997.

15. Schuette, J. C., Frank V Murphy IV, Kelley, C. A., Weir, J. R., Giesebrecht, J., Connell, S. R., Loerke, J., Mielke, T., Zhang, W., Penczek, P. A., Ramakrishnan, V., and Spahn, C. M. T., "GTPase Activation of Elongation Factor EF-Tu by the Ribosome During Decoding" *The EMBO Journal*, Vol. 28, pp. 755–765, 2009.

16. Staveley, B. E., "Principles of Cell Biology", http://www.mun.ca/biology/desmid /brian/BIOL2060/BIOL2060-22/2210.jpg, 2009.

17. Hauryliuk, V. V., "GTPases of the Prokaryotic Translation Apparatus", *Molecular Biology*, Vol. 40 (5), pp. 688–701, 2006.

18. Wieden, H. J., Gromadski K., Rodnin D., Rodnina M. V., "Mechanism of Elongation Factor (EF)-Ts Catalyzed Nucleotide Exchange in EF-Tu. Contribution of Contacts at the Guanine Base", *J. Biol. Chem.*, Vol. 277, pp. 6032–6036, 2002.

19. Andersen, G. R., Nissen, P. and Nyborg, J., "Elongation Factors in Protein Biosynthesis", *Trends in Biochemical Sciences*, Vol. 28 (8), pp. 434-441, 2003.

20. Kjeldgaard, M., Nissen, P., Thirup, S. and Nyborg, J., "The Crystal Structure of Elongation Factor EF-Tu from Thermus Aquaticus in the GTP Conformation", *Structure*, Vol. 1, pp. 35-50, 1993.

21. Polekhina, G., Thirup, S., Kjeldgaard, M., Nissen, P., Lippmann, C., Nyborg, J., "Helix Unwinding in the Effector Region of Elongation Factor Tu-GDP", *Structure*, Vol. 4 (10), pp. 1141-1151, 1996.

22. Nissen, P. et al., "The Crystal Structure of Cys-tRNACys:EFTu:GDPNP Reveals General and Specific Features in the Ternary Complex and in tRNA", *Structure*, Vol. 7, pp. 143–156, 1999.

23. Ahmadian, M. R., Kreutzer, R., Blechschmidt, B. and Sprinzl, M., "Site Directed Mutagenesis of Thermus Thermophilus EF-Tu: The Substitution of Threonine 62 by Serine and Alanine", *FEBS Letters*, Vol. 377, pp. 253-257, 1995.

24. Bourne, H. R., Sanders, D. A. and McCormick, F., "The GTPase Superfamily - Conserved Structure and Molecular Mechanism", *Nature*, Vol. 349, pp. 117-127, 1991.

25. Krab, I. M., and Andrea Parmeggiani, "Functional-Structural Analysis of Threonine 25, a Residue Coordinating the Nucleotide-bound Magnesium in Elongation Factor Tu", *The Journal of Biological Chemistry*, Vol. 274 (26), pp. 1132-1138, 1999.

26. Krab, I. M. and Parmeggiani, A., "Mutagenesis of Three Residues, Isoleucine-60, Threonine-61, and Aspartic Acid-80, Implicated in the GTPase Activity of

Escherichia coli Elongation Factor Tu", *Biochemistry*, Vol. 38, pp. 13035-13041, 1999.

27. Zeidler, W., Egle, C., Ribeiro, S., Wagner, A., Katunin, V., Kreutzer, R., Rodnina, M., Wintermeyer, W. and Sprinzl, M., "Site-directed mutagenesis of Thermus thermophilus elongation factor Tu Replacement of His85, Asp81 and Arg300", *Eur. J. Biochem.*, Vol. 229, pp. 596-604, 1995.

28. Scheidig, A. J., Burmester, C. and Goody, S. R., "The Pre-hydrolysis State of p21ras in Complex with GTP: New Insights into the Role of Water Molecules in the GTP Hydrolysis Reaction of Ras-like Proteins" *Structure*, Vol.7, pp. 1311–1324, 1999.

29. Knudsen, C. R. and Clark, B. F. C., "Site Directed Mutagenesis of Arg58 and Asp86 of Elongation Factor Tu From Escherichia coli: Effects on the GTPase Reaction and Aminoacyl-tRNA Binding, *Protein Engineering*, Vol. 8 (12), pp. 1267-1273, 1995.

30. Zeidler, W. et. al., "Limited Hydrolysis and Amino Acid Replacements in the Effector Region of *Thermus thermophilus* Elongation Factor Tu", *Eur. J. Biochem.*, Vol. 239, pp. 265-271, 1996.

31. Vogeley, L. et. al., "Conformational Change of Elongation Factor-Tu (EF-Tu) Induced by Antibiotic Binding. Crystal Structure of the Complex between EF-Tu·GDP and Aurodox." *J. Biol. Chem.*, Vol. 276, pp. 17149-17155, 2001.

32. Scarano, G., Krab, I. M., Bocchini, V. and Parmeggiani, A., "Relevance of Histidine 84 in the Elongation Factor Tu GTPase Activity and in Poly(Phe) Synthesis: Its Substitution by Glutamine and Alanine", *FEBS Letters*, Vol. 365, pp. 214-218, 1995.

33. Schweins, T., Geyer, M., Scheffzek, K., Warshel, A., Kalbitzer, H. R. and Wittinghofer, A. "Substrateassisted Catalysis as a Mechanism for GTP Hydrolysis

of p21ras and other GTP-binding Proteins. *Nature Struct. Biol.*, Vol. 2, pp. 36–44, 1995.

34. Grigorenko, B. L., Shadrina, M. S., Topol, I. A., Collins, J. R., Nemukhin, A. V., "Mechanism of the Chemical Step for the Guanosine triphosphate (GTP) Hydrolysis Catalyzed by Elongation Factor-Tu" *Biochimica et Biophysica Acta*, Vol. 1784, pp. 1908–1917, 2008.

35. Daviter, T., Wieden, H. J. and Rodnina, M. V., "Essential Role of Histidine 84 in Elongation Factor Tu for the Chemical Step of GTP Hydrolysis on the Ribosome", *J. Mol. Bio.*, Vol. 332, pp. 689-699, 2003.

36. Hilgenfeld, R., "Regulatory GTPases", *Curr. Opin. Struct. Biol.*,Vol. 5, pp. 810–817, 1995.

37. Jacquet, E. and Parmeggiani, A. "Substitution of Val20 by Gly in Elongation factor Tu. Effects on the Interaction with Elongation Factors Ts, Aminoacyl-tRNA and Ribosomes", *Eur. J. Biochem.*, Vol. 185, pp. 341-346, 1989.

38. Karplus, M. and McCammon, A. J., "Molecular Dynamics Simulations of Biomolecules", *Nature Structural Biology*, Vol. 9 (9), pp. 646-652, 2002.

39. Boyd, D. B., Lipkowitz, K. B., "Molecular Mechanics - The Method and Its Underlying Philosophy", *J. Chem. Ed.*, Vol. 59, pp. 269-274, 1982.

40. Rappe, A. K., Casewit, C. J., Colwell, K. S., Goddard III, W. A., Skiff, W. M., "UFF, A Full Periodic-Table Force-Field For Molecular Mechanics and Molecular-Dynamics Simulations", *J. Am. Chem. Soc.*, Vol. 114, pp. 10024-10035, 1992.

41. Cramer, C., *Essentials of Computational Chemistry: Theories and Models*, John Wiley & Sons: New York, 2002.

42. Leach, A. R., *Molecular Modelling: Principles and Applications*, (2nd edition), Prentice Hall, 2001.

43. Case, D. A., Darden, T. A., Cheatham, T. E., III, Simmerling, C. L., Wang, J., Duke, R. E., Luo, R., Crowley, M., Walker, R. C., Zhang, W., Merz, K. M., Wang, B., Hayik, S., Roitberg, A., Seabra, G., Kolossváry, I., Wong, K. F., Paesani, F., Vanicek, J., Wu, X., Brozell, S. R., Steinbrecher, T., Gohlke, H., Yang, L., Tan, C., Mongan, J., Hornak, V., Cui, G., Mathews, D. H., Seetin, M. G., Sagui, C., Babin, V. and P.A. Kollman, P. A., *AMBER 10*, University of California, San Francisco, 2008.

44. Duan, Y., Wu, C., Chowdhury, S., Lee, M. C., Xiong, G., Zhang, W., Yang, R., Cieplak, P., Luo, R. and Lee, T. "A Point-Charge Force Field for Molecular Mechanics Simulations of Proteins", *J. Comput. Chem.*, Vol . 24, pp. 1999-2012, 2003.

45. Hornak, V., Abel, R., Okur, A., Strockbine, B., Roitberg, A. and Carlos Simmerling, C., "Comparison of Multiple Amber Force Fields and Development of Improved Protein Backbone Parameters", *PROTEINS: Structure, Function, and Bioinformatics*, Vol. 65, pp. 712–725, 2006.

46. Meagher, K. L., Redman L. T. and Carlson, H. A., "Development of Polyphosphate Parameters for Use with the AMBER Force Field", *J. Comp. Chem.*, Vol. 24, pp. 1016-1025, 2003

47. Jorgensen, W. L., Chandrasekhar, J., Madura, J. D., Impey R. W. and Klein, M. L., "Comparison of Simple Potential Functions for Simulating Liquid Water", *J. Chem. Phys.*, Vol. 79, pp. 926-935, 1983.

48. Adcock, S. A. and McCammon, J. A., "Molecular Dynamics: Survey of Methods for Simulating the Activity of Proteins", *Chem. Rev.*, Vol. 106, pp. 1589-1615, 2006.

49. Berendsen, H.J.C., et al., “Molecular-Dynamics with Coupling to an External Bath”, *Journal of Chemical Physics*, Vol. 81 (8), pp. 3684-3690, 1984.

50. Adelman, S. A. and Doll, J. D., “Generalized Langevin Equation Approach for Atom-Solid Surface Scattering - General Formulation for Classical Scattering Off Harmonic Solids”, *Journal of Chemical Physics*, Vol. 64(6), pp. 2375-2388, 1976.

51. Ryckaert, J.-P.; Ciccotti, G.; Berendsen, H. J. C., “Numerical Integration of Cartesian Equations of Motion of a System with Constraints-Molecular Dynamics of N-Alkanes”, *J Comput Phys*, Vol. 23, pp. 327-341, 1977

52. Kräutler, V., van Gunsteren, W. F., Hünenberger, H. P., “A Fast SHAKE Algorithm to Solve Distance Constraint Equations for Small Molecules in Molecular Dynamics Simulations”, *Journal of Computational Chemistry*, Vol. 22, (5), pp. 501–508, 2001.

53. Knudsen, R. C. and Clark, F. C. B., “Site-directed Mutagenesis of Arg58 and Asp86 of Elongation Factor Tu from Escherichia coli: Effects on the GTPase Reaction and Aminoacyl-tRNA Binding”, *Protein Engineering*, Vol. 8 (12), pp. 1267-1273, 1995.

54. Liang, Z., Mather, T. and Li, G., “GTPase Mechanism and Function: New Insights from Systematic Mutational Analysis of the Phosphate-binding Loop Residue Ala30 of Rab5”, *Biochem. J.*, Vol. 346, pp. 501–508, 2000.

55. Cojocari, D., “Twenty-One Amino Acids”, http://upload.wikimedia.org/wikipedia/commons/thumb/3/37/Aa.svg/1000px-Aa.svg.png, 2010.